

Merging dynamical and structural indicators to measure resilience in multispecies systems

Lucas P. Medeiros¹  | Chuliang Song^{1,2,3}  | Serguei Saavedra¹ 

¹Department of Civil and Environmental Engineering, Massachusetts Institute of Technology, Cambridge, MA, USA

²Department of Biology, Quebec Centre for Biodiversity Science, McGill University, Montreal, Quebec, Canada

³Department of Ecology and Evolutionary Biology, University of Toronto, Toronto, Ontario, Canada

Correspondence
Serguei Saavedra
Email: sersaa@mit.edu

Funding information
National Science Foundation, Grant/Award Number: DEB-2024349

Handling Editor: Daniel Stouffer

Abstract

1. Resilience is broadly understood as the ability of an ecological system to resist and recover from perturbations acting on species abundances and on the system's structure. However, one of the main problems in assessing resilience is to understand the extent to which measures of recovery and resistance provide complementary information about a system. While recovery from abundance perturbations has a strong tradition under the analysis of dynamical stability, it is unclear whether this same formalism can be used to measure resistance to structural perturbations (e.g. perturbations to model parameters).
2. Here, we provide a framework grounded on dynamical and structural stability in Lotka–Volterra systems to link recovery from small perturbations on species abundances (i.e. dynamical indicators) with resistance to parameter perturbations of any magnitude (i.e. structural indicators). We use theoretical and experimental multispecies systems to show that the faster the recovery from abundance perturbations, the higher the resistance to parameter perturbations.
3. We first use theoretical systems to show that the return rate along the slowest direction after a small random abundance perturbation (what we call full recovery) is negatively correlated with the largest random parameter perturbation that a system can withstand before losing any species (what we call full resistance). We also show that the return rate along the second fastest direction after a small random abundance perturbation (what we call partial recovery) is negatively correlated with the largest random parameter perturbation that a system can withstand before at most one species survives (what we call partial resistance). Then, we use a dataset of experimental microbial systems to confirm our theoretical expectations and to demonstrate that full and partial components of resilience are complementary.
4. Our findings reveal that we can obtain the same level of information about resilience by measuring either a dynamical (i.e. recovery) or a structural (i.e. resistance) indicator. Irrespective of the chosen indicator (dynamical or structural), our results show that we can obtain additional information by separating the indicator into its full and partial components. We believe these results can motivate new theoretical approaches and empirical analyses to increase our understanding about risk in ecological systems.

Lucas P. Medeiros and Chuliang Song contributed equally.

KEY WORDS

dynamical stability, feasibility, microbial systems, recovery, resistance, species composition, structural stability

1 | INTRODUCTION

Ecological systems such as bird species competing for resources (Gibbs & Grant, 1987), plants and their mutualistic pollinators (Burkile et al., 2013) and microbes interacting in the human gut (Costello et al., 2012) face constant perturbations in changing environments. The *resilience* of such systems to different types of perturbations has been one of the most debated concepts in ecological research and has important implications for biodiversity and ecosystem functioning (Folke et al., 2016; Hodgson et al., 2015; Pimm et al., 2019). Broadly, resilience has been referred to as the ability of an ecological system to resist and recover from external perturbations (Capdevila et al., 2020; Hodgson et al., 2015). To understand these concepts and measures, epistemological work has established three necessary conditions to study ecological responses to perturbations (Justus, 2013): (a) a description of the ecological system, which mathematically takes the form of a *population dynamics model*, (b) the definition of a *reference state* from which the system will be perturbed, and (c) the definition of the type and magnitude of *perturbations*, which can act on state variables, model parameters (i.e. the system's structure) or both (see Glossary). Following this rationale, *recovery* (although it has also been called resilience, see Justus (2013) and Pimm et al. (2019)) has been typically defined as how fast a system returns to a reference state after a given perturbation (Capdevila et al., 2020; Hodgson et al., 2015). In turn, *resistance* has been defined as how much change a system can exhibit after a given perturbation (Capdevila et al., 2020; Hodgson et al., 2015). Hence, a sufficient condition for a system to be resilient is to exhibit fast recovery and high resistance. However, in order to assess the resilience of a system, it is paramount to have informative indicators of recovery and resistance and to understand the interconnection between these two measures, which may not necessarily be complementary (i.e. provide different qualitative information about the resilience of a system; Domínguez-García et al., 2019; Kéfi et al., 2019).

Recovery has had a strong tradition in the mathematical analysis of *asymptotic dynamical stability* (hereafter dynamical stability; Strogatz, 1994). In ecology, recovery has been typically conceptualized as the return rate along the slowest direction to a reference equilibrium state (Dakos et al., 2015; Donohue et al., 2016; Pimm & Lawton, 1977). This return rate can be quantified by the real part of the largest eigenvalue (if negative) of the Jacobian matrix when evaluated at equilibrium (Logofet, 2018; Novak et al., 2016). The Jacobian matrix represents the linearized dynamical forces acting around a given state. This implies that recovery has been mathematically quantified by the long-term return rate (or the return time if inverted) of a system to a reference equilibrium state after small perturbations (per the linear validity of the Jacobian) acting on species abundances (i.e. the state variables of the system).

By contrast, the measurement of resistance has had a weaker tradition in the field of dynamical systems (Strogatz, 1994) and it is unclear whether it can be linked to dynamical stability in ecological systems (Domínguez-García et al., 2019; Justus, 2013). Resistance has been typically quantified as the magnitude of displacement of a system following a perturbation (Carpenter et al., 1992; Hillebrand et al., 2018). Differently from recovery, resistance is not necessarily limited to a particular quantitative equilibrium state (i.e. abundance distribution at equilibrium), and it is expected to reflect the response of a system to perturbations acting on both species abundances and on the structure of a system (Donohue et al., 2016; Pimm et al., 2019). Formally, this structure can be represented by a population dynamics model describing the governing laws of a system and its parameters (Justus, 2013). That is, while species abundances represent the state variables of a system, the structure represents the model parameters (and the model itself). Thus, it remains unclear whether recovery from abundance perturbations and resistance to structural perturbations can be quantified within the same formalism, and whether there are potential connections between these two aspects of resilience (Hodgson et al., 2015; Pimm et al., 2019).

Focusing on parameter perturbations, a dynamical system is said to be *structurally stable* if the topology of the phase portrait (i.e. the qualitative behaviour of a dynamical system) is preserved under smooth parameter changes (Smale, 1967; Arnold, 1988). For example, a system with S species can be considered structurally stable if none of the species goes extinct after small changes in the parameters corresponding to species intrinsic growth rates (Saavedra et al., 2017). Importantly, it has already been shown that the sensitivity to stochastic perturbations of abundances in the vicinity of an equilibrium is equivalent to the sensitivity to fluctuations of the parameters within the same vicinity (Arnoldi & Haegeman, 2016). Specifically, the response to external infinitesimal perturbations acting on species abundances agrees with the minimal parameter perturbation able to render the system dynamically unstable. Furthermore, structurally unstable systems (i.e. systems that change their qualitative behaviour after small parameter changes) are characterized by conditions under which the largest eigenvalue of the Jacobian matrix is equal to zero (Duan, 2015; Strogatz, 1994). These previous results have established a potential direction to link *dynamical indicators* (i.e. measures related to perturbations acting on species abundances) with *structural indicators* (i.e. measures related to perturbations acting on model parameters) to measure resilience in ecological systems (Cenci & Saavedra, 2018; Constable & McKane, 2015; Dobrinevski & Frey, 2012).

Here, we extend the connection between dynamical and structural indicators beyond the vicinity of an equilibrium state to study resilience in multispecies ecological systems. Specifically,

GLOSSARY

Asymptotic dynamical stability: The capacity of a dynamical system to return to a quantitative equilibrium reference state after a given perturbation acting on its state variables (i.e. species abundances; Strogatz, 1994).

Dynamical indicator: A measure of resilience related to perturbations acting on species abundances.

Feasibility domain: The set of directions of parameter values (here intrinsic growth rates) compatible with positive solutions for all species (i.e. feasible system).

Full recovery: The return rate along the slowest direction following a perturbation acting on species abundances. We measure full recovery as the largest eigenvalue (λ_1) of the Jacobian matrix evaluated at an equilibrium state.

Full resilience: The capacity of a system to maintain its full species composition through the recovery and resistance of all species. Full resilience is partitioned into full recovery, which is related to abundance perturbations (i.e. asymptotic dynamical stability), and full resistance, which is related to parameter perturbations (i.e. structural stability).

Full resistance: The largest random parameter perturbation that the system can withstand before losing any species. We measure full resistance as the distance of an equilibrium state to the closest border ($\min\{d_b\}$) of the feasibility domain ($D_F(\mathbf{A})$).

Partial recovery: The return rate along the second fastest direction following a perturbation acting on species abundances. We measure partial recovery as the second smallest eigenvalue (λ_{S-1}) of the Jacobian matrix evaluated at an equilibrium state.

Partial resilience: The capacity of a system to maintain a partial species composition through the recovery and resistance of a subset of species. Partial resilience is partitioned into partial recovery, which is related to abundance perturbations (i.e. asymptotic dynamical stability), and partial resistance, which is related to parameter perturbations (i.e. structural stability).

Partial resistance: The largest random parameter perturbation that a system can withstand before at most a single species survives. We measure partial resistance as the distance of an equilibrium state to the closest vertex ($\min\{d_v\}$) of the feasibility domain ($D_F(\mathbf{A})$).

Perturbation: Any event that impacts the species abundances directly or the rules that govern population dynamics in an ecological system (i.e. the structure of the ecological system; Justus, 2013).

Population dynamics model: A mathematical idealized description of the causal relationships (mechanistic or phenomenological) connecting the change of a population through time as a function of abiotic and biotic factors (Case, 2000).

Recovery: The rate of return (or time, if inverted) of an ecological system to a reference state after a given perturbation (Hodgson et al., 2015).

Reference state: The state of an ecological system against which the perturbed system will be compared to (Justus, 2013). The reference state can be quantitative (e.g. the species abundances at equilibrium) or qualitative (e.g. the species composition of the system).

Resilience: Ability of an ecological system (i.e. set of interacting species) to resist and recover from external perturbations (Hodgson et al., 2015).

Resistance: The capacity of an ecological system to resist changes in relation to its reference state after a given perturbation (Hodgson et al., 2015).

Structural indicator: A measure of resilience related to perturbations acting on model parameters.

Structural stability: The capacity of a dynamical system to retain the topology of the phase portrait (i.e. the qualitative behavior of the trajectories) after a given perturbation to its structure (i.e. governing laws or model parameters; Strogatz, 1994).

we link recovery with dynamical stability and define it as the long-term return rate of a system to a quantitative reference state (i.e. abundance distribution at equilibrium) after small random perturbations on species abundances. We then separate recovery into *full* and *partial recovery* as to whether species abundances return fully or partially to such quantitative reference state respectively. Next, we link resistance with structural stability and define it as the ability of a system to remain in a qualitative reference state (i.e. species composition at equilibrium) after random parameter perturbations of any magnitude. We then separate resistance into *full* and *partial resistance* as to whether all the species or at most one species remains in such qualitative reference state respectively. Therefore, we define *full resilience* as the capacity of a system to maintain its full species composition through the recovery

and resistance of all species. Then, we define *partial resilience* as the capacity of a system to maintain a partial species composition through the recovery and resistance of a subset of species (see Glossary).

We first illustrate our framework using theoretically parameterized ecological systems spanning multiple interaction types and number of species. In particular, we explore competition, mutualistic and antagonistic systems with 3, 4 and 5 species. Overall, we find that when considering abundance and parameter perturbations together, recovery and resistance are interconnected measures of resilience. However, we show that these dynamical and structural indicators can provide complementary information about a system when separated into full and partial resilience. Then, we apply our framework to 17 experimentally parameterized

microbial systems containing three interacting species each. We corroborate our theoretical results that full and partial resilience are complementary components of experimental systems. Finally, we discuss the implications of our findings and future avenues of research on resilience.

2 | MATERIALS AND METHODS

2.1 | Population dynamics model

To study and measure resilience in ecological systems, it is necessary to define (a) a population dynamics model, (b) a reference state, and (c) the system's response as a function of the type and magnitude of perturbations (Justus, 2013). Focusing on the model, we assume that the dynamics of ecological systems are governed by any model topologically equivalent to the classic Lotka–Volterra (LV) dynamics. It has been shown that if the unstable and stable equilibria of the classic LV model can be mapped into the unstable and stable equilibria of a modified model, then this modified model is topologically equivalent to the classic LV (Cenci & Saavedra, 2018; Saavedra et al., 2020). The classic LV model written in the r-formalism is given by (Case, 2000):

$$\frac{dN_i}{dt} = N_i \left(r_i + \sum_{j=1}^S a_{ij} N_j \right), i = 1, \dots, S, \quad (1)$$

where N_i is the abundance (or biomass) of species i , S is the number of species in the system and a_{ij} is an element of the interaction matrix $\mathbf{A} = \{a_{ij}\}$ representing the per capita effect of species j on species i . The phenomenological parameter r_i is the intrinsic growth rate of species i , representing how abiotic factors affect the balance between mortality and resource intake (Case, 2000; Coulson et al., 2017).

To investigate resilience in the classic LV model, we generate fully connected random interaction matrices \mathbf{A} by setting the diagonal elements to $a_{ii} = -1\forall i$ (introducing the biological principle of self-regulation), whereas the off-diagonal elements a_{ij} ($i \neq j$) are randomly drawn from a normal distribution with mean zero and variance σ^2 (i.e. $a_{ij} \sim \mathcal{N}(0, \sigma^2)$). Note that the value of σ^2 sets the relative strength of interspecific interactions (a_{ij}) given that intraspecific interactions are fixed (i.e. $a_{ii} = -1$). To explore different types of ecological systems, we introduce sign constraints: (i) $a_{ij} < 0$ for competition systems, (ii) $a_{ij} > 0$ for mutualistic systems, and (iii) $a_{ij}a_{ji} < 0$ for antagonistic systems (Allesina & Tang, 2012; Murdoch et al., 2003; see *Resilience in theoretical ecological systems*). Applying these constraints is equivalent to sampling a_{ij} from a half-normal distribution and taking the appropriate sign reversal (Allesina & Tang, 2012; Song et al., 2020). For simplicity, we only explore one type of antagonistic network structure given by a matrix \mathbf{A} where $a_{ij} < 0$ if $i > j$ and $a_{ij} > 0$ if $i < j$ (e.g. a trophic chain with omnivory). Note that, in these antagonistic systems, the feasibility condition itself (i.e. $N_i^* > 0\forall i$; see Reference state) constrains the r_i values to be ecologically realistic as top

predators and producers would necessarily have negative and positive r_i values respectively.

To guarantee that reference equilibrium states are dynamically stable (see Reference state), we follow a probabilistic criteria for random matrices and set the variance of the distribution of interaction strengths proportional to system size ($\sigma^2 = 1/S^2$; May, 1972). Note that having σ^2 to scale with the number of species S is an ecologically realistic assumption (Dougoud et al., 2018). We also tested a scenario in which interspecific interactions are stronger (i.e. $\sigma^2 = 1/S$) and obtained similar results (Figures S3 and S4). It is important to note that, under our framework, we cannot increase the relative strength of interspecific interactions beyond a certain limit in order to guarantee dynamical stability. Thus, we assume that every species in our theoretical systems (see *Resilience in theoretical ecological systems*) is self-regulated, including predators in antagonistic systems (Barabás et al., 2017; Song & Saavedra, 2020).

2.2 | Reference state

We consider a feasible and dynamically stable equilibrium as our reference state (Song et al., 2020; Song & Saavedra, 2018). Feasibility corresponds to the capacity of a system to sustain all its constituent species over the long run. Formally, feasibility implies the existence of a positive solution (i.e. $N_i^* > 0\forall i$ under the equilibrium $dN_i/dt = 0$ in Equation 1). Note that feasibility is a necessary condition for persistence, permanence and the existence of bounded orbits (Hofbauer & Sigmund, 1998). In turn, we define dynamical stability as the capacity of a system to return to its feasible equilibrium state after small random perturbations on species abundances. This is fulfilled when all the eigenvalues of the Jacobian matrix (\mathbf{J}) when evaluated at the equilibrium state ($\mathbf{N}^* = [N_1^*, \dots, N_S^*]^T$, as defined by $d\mathbf{N}^*/dt = 0$) have negative real parts (Case, 2000; May, 1972).

For the classic LV dynamics (Equation 1), the Jacobian matrix at a feasible equilibrium is defined as:

$$\mathbf{J} = \text{diag}(\mathbf{N}^*) \cdot \mathbf{A}, \quad (2)$$

where $\text{diag}(\mathbf{N}^*)$ is a diagonal matrix with N_1^*, \dots, N_S^* in its diagonal. The equilibrium of the classic LV model is given by the vector of species abundances $\mathbf{N}^* = -\mathbf{A}^{-1}\mathbf{r}$. This definition of reference state has the advantage of allowing us to represent it as a quantitative or qualitative reference state. Quantitatively, the focus is on the exact values of the feasible and dynamically stable equilibrium \mathbf{N}^* (i.e. the species abundance distribution at equilibrium). Qualitatively, the focus is on the existence of such a feasible equilibrium ($N_i^* > 0\forall i$; i.e. the species composition at equilibrium).

2.3 | Recovery from abundance perturbations

Regarding the response of a system to abundance perturbations, we focus on the standard definition of recovery linked to dynamical

stability (Strogatz, 1994). Specifically, we define recovery as the return rate of a system to a feasible and dynamically stable reference state after a small perturbation on abundances. Formally, we use as indicators the real part of the largest (λ_1) and second smallest (λ_{S-1}) eigenvalues of the Jacobian matrix (J) evaluated at equilibrium (Equation 2). The largest eigenvalue (if negative) measures the return rate along the slowest direction of recovery. Because species abundances will have recovered completely after going through the slowest direction, we use λ_1 as an indicator of full recovery. The second smallest eigenvalue (if negative) represents the return rate along the second fastest direction. Because species abundances will have only partially recovered after going through the second fastest direction, we use λ_{S-1} as an indicator of partial recovery. Thus, for each possible feasible and dynamically stable state (\mathbf{N}^*) of a system, we use λ_1 and λ_{S-1} as a measure of its full and partial recovery respectively (Figure 1a,b). To be able to compare

λ_1 and λ_{S-1} across different equilibrium states, we normalize \mathbf{N}^* to unit norm (i.e. $\|\mathbf{N}^*\| / |\mathbf{N}^*| = 1$) before computing these indicators.

2.4 | Resistance to parameter perturbations

Shifting our focus to the response of a system to random parameter perturbations of any magnitude, we base our analysis on the concept of structural stability and link it with resistance. We define resistance as the smallest random parameter perturbation that a system can tolerate without affecting its qualitative reference state (defined as a feasible and dynamically stable equilibrium). For a given interaction matrix A , feasibility in the classic LV model will be satisfied as long as the r -vector falls inside the *feasibility domain* defined as (Medeiros et al., 2021; Song et al., 2018):

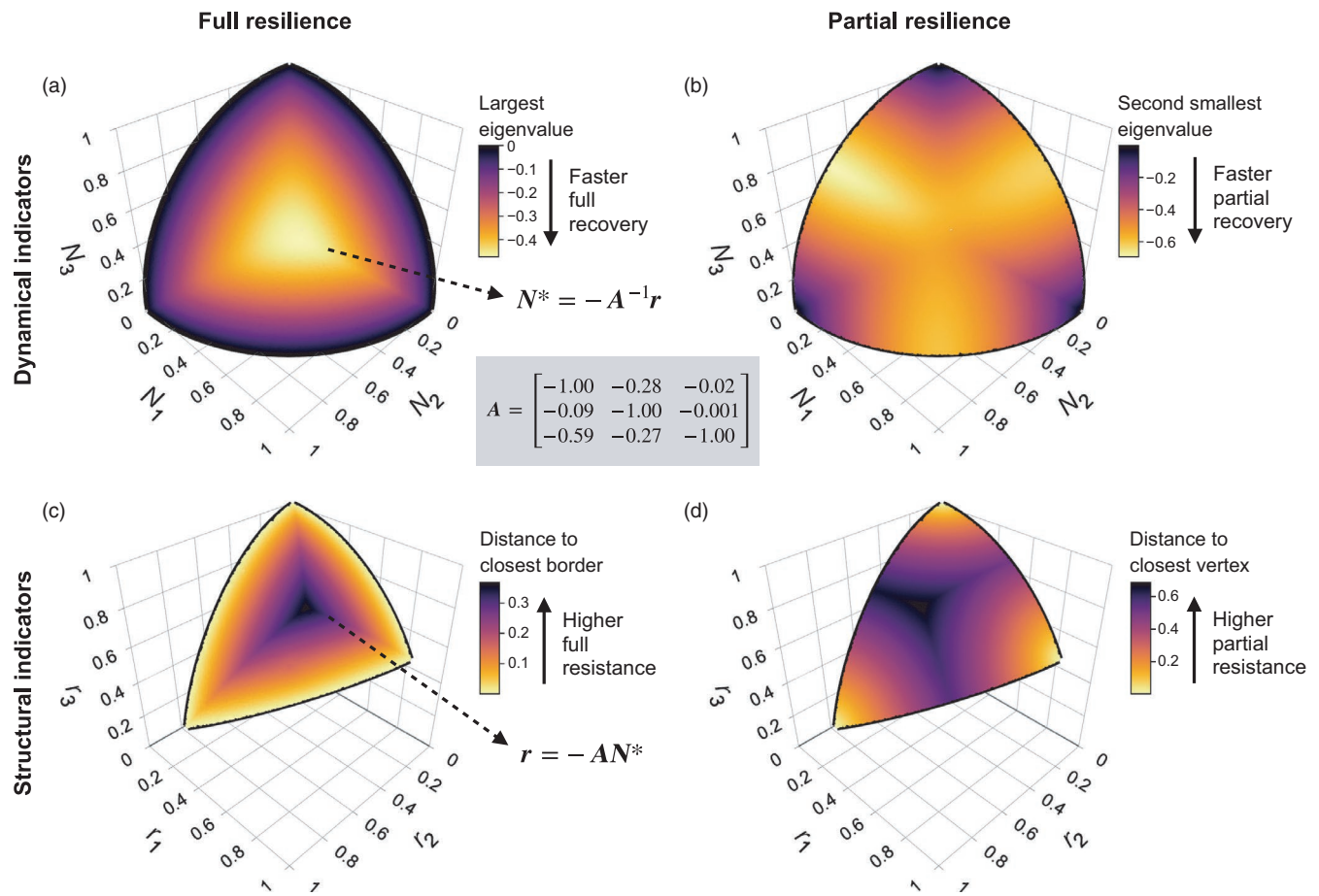


FIGURE 1 Dynamical and structural indicators of full and partial resilience. (a) An illustrative example of a 3-dimensional space of species abundances at equilibrium ($\mathbf{N}^* = [N_1^*, N_2^*, N_3^*]^T$) coloured according to the largest eigenvalue (λ_1) of the Jacobian matrix (J) evaluated at equilibrium. The interaction matrix A of this 3-species competition system is shown in the centre of the figure. Lower values of λ_1 indicate a faster full recovery of the system after abundance perturbations. Note that this space corresponds to the positive orthant of the unit sphere (i.e. $\|\mathbf{N}^*\| = 1, N_i^* > 0 \forall i$). (b) The same space of species abundances, but coloured according to the second smallest eigenvalue (λ_2) of J evaluated at equilibrium. Lower values of λ_2 indicate a faster partial recovery after abundance perturbations. (c) The space of intrinsic growth rates ($\mathbf{r} = [r_1, r_2, r_3]^T$) for the same system shown in (a) and (b) coloured according to the distance to closest border ($\min\{d_b\}$) of the feasibility domain ($D_F(A)$), which are indicated as black curves. Higher values of $\min\{d_b\}$ indicate a higher full resistance to perturbations on intrinsic growth rates. Note that \mathbf{r} -vectors on the feasibility domain are normalized to unit norm (i.e. $\|\mathbf{r}\| = 1$). (d) The same space of intrinsic growth rates, but coloured according to the distance to closest vertex ($\min\{d_v\}$) of $D_F(A)$. Higher values of $\min\{d_v\}$ indicate a higher partial resistance to perturbations on intrinsic growth rates.

$$D_F(\mathbf{A}) = \{\mathbf{r} \in \mathbb{R}^S \mid \mathbf{r} = N_1^* \mathbf{v}_1 + \dots + N_S^* \mathbf{v}_S, \text{with } N_1^*, \dots, N_S^* > 0\}, \quad (3)$$

where $-\mathbf{v}_i$ is the i th column vector of \mathbf{A} and N_i^* is the feasible (i.e. positive) abundance of species i at equilibrium. Geometrically, $D_F(\mathbf{A})$ is a cone in S dimensions and any \mathbf{r} -vector inside the cone gives rise to a feasible solution. Note that only the direction of the \mathbf{r} -vector matters because if Equation (3) is satisfied for a given vector \mathbf{r} , it is also satisfied for a scaled vector $c\mathbf{r} \forall c > 0$. Therefore, the region inside the borders of $D_F(\mathbf{A})$ corresponds to the specific directions of \mathbf{r} for which the system is feasible (Saavedra et al., 2017). Ecologically, this domain defines the range of conditions linked to abiotic factors, which are phenomenologically represented by the direction of the \mathbf{r} -vector, compatible with the persistence of all species in the system characterized by \mathbf{A} (Medeiros et al., 2021; Song et al., 2020). Note that we do not impose any restriction on the sign of the elements r_i of the \mathbf{r} -vector, they can be positive or negative depending on $D_F(\mathbf{A})$ (Song et al., 2018).

Importantly, starting from a feasible equilibrium state \mathbf{N}^* , a border of $D_F(\mathbf{A})$ (i.e. $\mathbf{r} = \sum_{i=1}^S N_i^* \mathbf{v}_i$ with $N_j^* = 0$ and $N_i^* > 0 \forall i \neq j$) represents a limit in the direction of \mathbf{r} where at least one of the S species (i.e. species j) goes extinct (Grilli et al., 2017; Rohr et al., 2016; Tabi et al., 2020). Similarly, a vertex of $D_F(\mathbf{A})$ (i.e. $\mathbf{r} = N_i^* \mathbf{v}_i$ with $N_i^* > 0$ and $N_j^* = 0 \forall j \neq i$) represents a limit in the direction of \mathbf{r} where a single species (i.e. species i) survives at most, depending on whether this species is self-sustained (Grilli et al., 2017; Rohr et al., 2016; Tabi et al., 2020). For example, with three species, if one sets $N_1^* = 0$, the \mathbf{r} -vector will lie on one of the borders of the cone ($D_F(\mathbf{A})$), which is given by $\mathbf{r} = N_2^* \mathbf{v}_2 + N_3^* \mathbf{v}_3$, with $N_2^*, N_3^* > 0$. Furthermore, if $N_1^* = 0$ and $N_2^* = 0$, then the \mathbf{r} -vector will lie on one of the vertices of $D_F(\mathbf{A})$, which is given by $\mathbf{r} = N_3^* \mathbf{v}_3$, with $N_3^* > 0$. Thus, we focus on the shortest distances that a system can withstand before hitting a border or vertex under random perturbations to \mathbf{r} . Note that we focus on random perturbations as we typically have no a priori information about the direction of environmental perturbations. Importantly, measuring such distances in the parameter space allows us to consider how resistant a system is to parameter perturbations of any magnitude.

Because it is only necessary to know the direction (not the magnitude) of \mathbf{r} to know if a system \mathbf{A} is feasible, we normalize the intrinsic growth rates to unit norm (i.e. $\mathbf{r}/|\mathbf{r}|$). Then, the distance between an intrinsic growth rate vector inside the feasibility domain ($\mathbf{r}(\mathbf{N}^*)$) and a border of $D_F(\mathbf{A})$ can be calculated by the arc length (i.e. angle) between $\mathbf{r}(\mathbf{N}^*)$ and $\mathbf{r}(\text{border})$ as: $d_b = \arccos(\mathbf{r}(\mathbf{N}^*) \cdot \mathbf{r}(\text{border}))$, where $\mathbf{r}(\text{border})$ is the orthogonal projection of $\mathbf{r}(\mathbf{N}^*)$ onto the border (Grilli et al., 2017). For a system with S species, each $\mathbf{r}(\mathbf{N}^*)$ inside the feasibility domain is associated with one distance to each of the $\binom{S}{S-1} = S$ borders. We focus on the distance to the closest border ($\min\{d_b\}$). Thus, the distance of a system to the closest border ($\min\{d_b\}$) represents the largest random parameter perturbation that the system can withstand before losing any species—which we call full resistance. Similarly, the distance between $\mathbf{r}(\mathbf{N}^*)$ and a vertex of $D_F(\mathbf{A})$ can be calculated by the arc length between $\mathbf{r}(\mathbf{N}^*)$ and $\mathbf{r}(\text{vertex})$ as: $d_v = \arccos(\mathbf{r}(\mathbf{N}^*) \cdot \mathbf{r}(\text{vertex}))$, where $\mathbf{r}(\text{vertex})$ is the

\mathbf{r} -vector associated with the vertex. Note that the \mathbf{r} -vector associated with a given vertex is equal to the corresponding column vector of \mathbf{A} scaled by the single species abundance at equilibrium (i.e., $\mathbf{r} = N_i^* \mathbf{v}_i$). For a system with S species, each $\mathbf{r}(\mathbf{N}^*)$ inside the feasibility domain is associated with one distance to each of the $\binom{S}{1} = S$ vertices. We focus on the distance to the closest vertex ($\min\{d_v\}$). Therefore, the distance of a system to the closest vertex ($\min\{d_v\}$) represents the largest random parameter perturbation that a system can withstand before it is reduced to at most a single species—which we call partial resistance (Figure 1c,d).

2.5 | Resilience in theoretical ecological systems

First, we investigate the potential associations between recovery and resistance according to our measures described above across several theoretical systems (i.e. matrices \mathbf{A}). To do so, we first generate three types of random matrices: competition systems, mutualistic systems and antagonistic systems (see *Population dynamics model*). For each of these three types of system, we generate 100 random matrices \mathbf{A} by sampling the interspecific interaction coefficients a_{ij} from $\mathcal{N}(0, \frac{1}{S^2})$ for three different system sizes: $S = 3, 4$ and 5 species. Then, for each random matrix, we sample $100 \times 2^{(S-2)}$ feasible equilibria (i.e., $\mathbf{N}^* > 0$) uniformly on the unit S -dimensional hypersphere (i.e. $||\mathbf{N}^*|| = 1$) and solve for the intrinsic growth rates: $\mathbf{r} = -\mathbf{A}\mathbf{N}^*$. To guarantee dynamical stability in addition to feasibility, we only sample equilibrium states for which the real part of the largest eigenvalue of $\mathbf{J} = \text{diag}(\mathbf{N}^*)\mathbf{A}$ is negative. We eliminate random matrices for which all sampled equilibrium states had a non-negative largest eigenvalue. Note that we increase the number of sampled equilibrium states exponentially with S to account for the fact that sparsity among points grows exponentially with the number of dimensions.

For each feasible and dynamically stable equilibrium state that we sample, we calculate its full recovery (largest eigenvalue, λ_1), partial recovery (second smallest eigenvalue, λ_{S-1}), full resistance (distance to closest border, $\min\{d_b\}$) and partial resistance (distance to closest vertex, $\min\{d_v\}$). To investigate whether recovery and resistance are linked, we compute the Pearson correlation coefficient (hereafter correlation) between full recovery and full resistance ($\rho(\lambda_1, \min\{d_b\})$), as well as the correlation between partial recovery and partial resistance ($\rho(\lambda_{S-1}, \min\{d_v\})$). We compute such correlations separately for each random system \mathbf{A} . A strong negative correlation indicates that the faster the recovery from abundance perturbations, the higher the resistance to parameter perturbations (Figure 1). Finally, we study the complementarity between our indicators by computing the partial correlation between λ_1 and λ_{S-1} controlling for the rank of λ_1 ($\rho(\lambda_1, \lambda_{S-1} | \text{rank of } \lambda_1)$). This control is necessary to account for the fact that $\lambda_1 \geq \lambda_{S-1}$ for each equilibrium state by definition. We also compute the partial correlation between $\min\{d_b\}$ and $\min\{d_v\}$ controlling for the rank of $\min\{d_v\}$ ($\rho(\min\{d_b\}, \min\{d_v\} | \text{rank of } \min\{d_v\})$). Note that $\min\{d_v\} \geq \min\{d_b\}$ for each equilibrium state. A value close to zero of these partial correlations would imply that full and partial components are complementary.

2.6 | Resilience in experimental microbial systems

Next, we investigate the complementarity and potential application of our indicators of resilience using experimental ecological systems. For this purpose, we use 17 feasible and dynamically stable systems where each system consists of three interacting soil-dwelling bacteria species (Friedman et al., 2017). These publicly available data come from a very detailed and controlled study performing persistence experiments by co-inoculating different combinations of heterotrophic soil-dwelling bacteria species at varying initial fractions and propagating them through five growth–dilution cycles (Friedman et al., 2017). Each 3-species experimental system is characterized by an interaction matrix \mathbf{A} and an intrinsic growth rate vector \mathbf{r} . The experimental values of \mathbf{r} were inferred by fitting via least-squares the classic LV model (Equation 1) to the observed abundance time series of species monocultures (Friedman et al., 2017; Table S1). Each interaction matrix \mathbf{A} was inferred through pairwise tournaments by fitting via least-squares Equation (1) to the observed time series of species abundances (Friedman et al., 2017; Table S2). Although more than 17 systems with three species are available from this dataset, we only use the systems for which the equilibrium state obtained using the experimentally inferred matrix \mathbf{A} and intrinsic growth rate vector \mathbf{r} ($\mathbf{N}^* = -\mathbf{A}^{-1}\mathbf{r}$) is feasible and dynamically stable (Table S3).

Importantly, interaction matrices contained competition interactions (i.e. $a_{ij}, a_{ji} < 0$), antagonistic interactions (i.e. $a_{ij} < 0, a_{ji} > 0$) or a mix of both. It is also important to note that the strength of inferred interactions (a_{ij}) varies greatly across and within experimental systems (Table S2), allowing us to test our framework for different scenarios of interaction strengths. For each of the 17 systems (each combination of \mathbf{A} and \mathbf{r}), we calculate its full and partial resilience components following the same methodology as described above (see *Resilience in theoretical ecological systems*). Additionally, for each experimental system, we randomly sampled 2,000 feasible and dynamically stable equilibria uniformly on the positive orthant of the unit sphere (i.e. $\mathbf{N}^* > 0, ||\mathbf{N}^*|| = 1$, and $\lambda_1 < 0$) and measured our resilience indicators for each one of these sampled equilibria. The rationale behind sampling these 2,000 random equilibria was to compare the full/partial recovery and full/partial resistance observed for the experimental systems with other potential values of these indicators that could have been observed under different conditions.

Following our analysis with theoretical systems, for each of the 17 experimental systems, we study the complementarity of our indicators by computing the partial correlation between full recovery and partial recovery (λ_1, λ_2) controlling for the rank of λ_1 ($\rho(\lambda_1, \lambda_2$ rank of λ_1)) as well as the partial correlation between full resistance and partial resistance ($\min\{d_b\}, \min\{d_v\}$) controlling for the rank of $\min\{d_v\}$ ($\rho(\min\{d_b\}, \min\{d_v\}$ rank of $\min\{d_v\}$)). Then, in order to properly summarize the relationship between full and partial resilience across systems, we compute a relative value for each indicator ($\tilde{\lambda}_1, \tilde{\lambda}_2, \min\{\tilde{d}_b\}$, and $\min\{\tilde{d}_v\}$) by dividing each indicator by its minimum (recovery indicators) or maximum (resistance indicators) possible value that can be attained inside its corresponding feasibility domain. For example, the relative value of λ_1 ($\tilde{\lambda}_1$) for a given experimental

equilibrium state \mathbf{N}^* is obtained by dividing λ_1 by the minimum value of λ_1 attained over all 2,000 randomly sampled equilibria \mathbf{N}^* , i.e. $\tilde{\lambda}_1 = \lambda_1 / \min\{\lambda_1\}$. Thus, relative values close to zero or one represent systems that have the minimum or maximum possible resilience respectively. It is worth highlighting that this normalization does not allow us (and it is not intended) to compare the level of resilience between two different systems, only their resilience relative to the maximum possible value within the feasibility domain of the given system. Thus, a large variation in the experimental values of relative full and partial resilience can indicate a strong heterogeneity of resilience patterns across systems.

3 | RESULTS

We found that fast recovery from abundance perturbations (i.e. state variables, N_i^*) is associated with a high resistance to parameter perturbations (i.e. perturbations on intrinsic growth rates, r_i). Specifically, we found a strong negative correlation between full recovery (largest eigenvalue, λ_1) and full resistance (distance to closest border, $\min\{d_b\}$) across the three types of theoretical ecological systems (competition, mutualistic and antagonistic systems; Figure 2a; Figures S1 and S2). Moreover, we found that this strong association between full recovery and full resistance holds for multiple random systems with different number of species (Figure 2b; Table S4). We obtained similar results for stronger interspecific interactions (i.e. $\sigma^2 = 1/S$), but correlations can be weaker due to a smaller variation in λ_1 and highly asymmetric feasibility domains (i.e. high variation among the border lengths; Figure S3). We can understand this result by noting that the Jacobian matrix associated with an \mathbf{r} -vector on a border of the feasibility domain will have a row of zeros, which implies that the largest eigenvalue of this matrix will be zero (Figure 1a). In particular, all elements of the i th row of the Jacobian will be zero when the system is located at the border where $N_i^* = 0$. Recall that all eigenvalues of the Jacobian matrix need to be negative in order to guarantee dynamical stability and more negative values imply faster recovery.

Similarly, we found a strong negative correlation between partial recovery (second smallest eigenvalue, λ_{S-1}) and partial resistance (distance to closest vertex, $\min\{d_v\}$) across the three types of theoretical systems (Figure 3a; Figures S1 and S2). In addition, we confirmed that this strong relationship between partial recovery and partial resistance holds for multiple random systems with different number of species (Figure 3b; Table S4), even when interspecific interactions are stronger (Figure S4). Similar to the association between λ_1 and $\min\{d_b\}$, the association between λ_{S-1} and $\min\{d_v\}$ can be understood by noting that the Jacobian matrix associated with an \mathbf{r} -vector on a vertex will have $S - 1$ rows of zeros. This implies that the largest $S - 1$ eigenvalues of the Jacobian will be zero at a vertex and, therefore, the second smallest eigenvalue will be associated with the distance to the closest vertex (Figure 1a,b).

We can additionally separate the relationship between recovery (full or partial) and resistance (full or partial) by the different

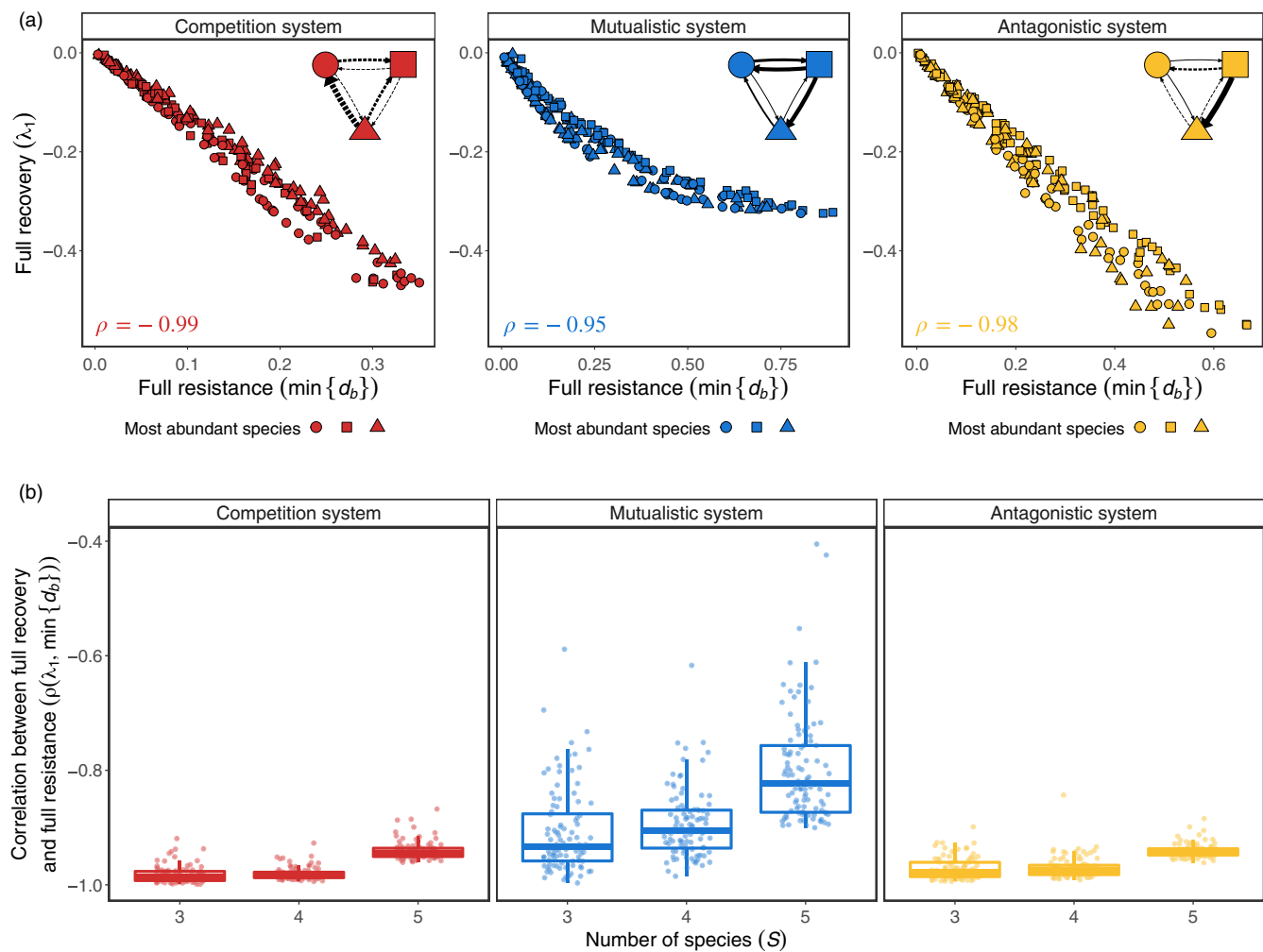


FIGURE 2 Relationship between full recovery and full resistance in theoretical systems. (a) Each panel shows 200 values of full recovery (largest eigenvalue, λ_1) and full resistance (distance to closest border, $\min\{d_b\}$) of one illustrative theoretical random system with three species (red: competition system, blue: mutualistic system, and yellow: antagonistic system). Interaction networks on the top right corner of each panel depict the interaction matrices A (dashed line: negative interaction, solid line: positive interaction, and line width: interaction strength). Point shapes (circle, square and triangle) correspond to the species with the highest abundance at that equilibrium state. Correlation values between λ_1 and $\min\{d_b\}$ are shown in the bottom left corner of each panel. The competition system is the same one as shown in Figure 1. (b) Each panel shows the correlation values between λ_1 and $\min\{d_b\}$ for a given type of system and for three system sizes ($S = 3, 4$, and 5). Boxplots denote the median and interquartile range and points show the actual correlation values obtained for each system type and size (100 values per boxplot corresponding to 100 theoretical systems)

vertices of the feasibility domain, noting that each vertex corresponds to the dominant species in the system (represented by different symbols in Figures 2a and 3a; Rohr et al., 2016; Tabi et al., 2020). The extent to which the relationship between recovery and resistance may differ across vertices depends on the level of asymmetry in the feasibility domain (Rohr et al., 2016; Tabi et al., 2020). However, regardless of the asymmetry in the feasibility domain or the identity of the most abundant species, the relationship between recovery and resistance remains strongly negative for each vertex (Figures 2a and 3a). To further explore this result, we computed the partial correlation between recovery and resistance while controlling for the identity of the most abundant species and, as expected, obtained slightly stronger correlation values for λ_{S-1} and $\min\{d_v\}$ but not for λ_1 and $\min\{d_b\}$

(Figures S5 and S6; Table S5). In addition, we also confirmed that our indicators of recovery (λ_1 and λ_{S-1}) and resistance ($\min\{d_b\}$ and $\min\{d_v\}$) are weakly correlated after controlling for the rank of the largest variable and, therefore, complement each other (Figures S7 and S8; Table S5).

Moving to the experimental data, we confirmed the negative correlation between full recovery (λ_1) and full resistance ($\min\{d_b\}$; Figure 4a) as well as between partial recovery (λ_2) and partial resistance ($\min\{d_v\}$; Figure 4b) using 3-species microbial systems. In particular, we found that $\rho(\lambda_1, \min\{d_b\})$ and $\rho(\lambda_2, \min\{d_v\})$ are strong and negative for all 17 experimental systems (Figure 4c; Tables S6 and S7). Thus, the interconnections between recovery and resistance remained strong for the experimental systems despite large differences in the type of interactions (i.e. competition,

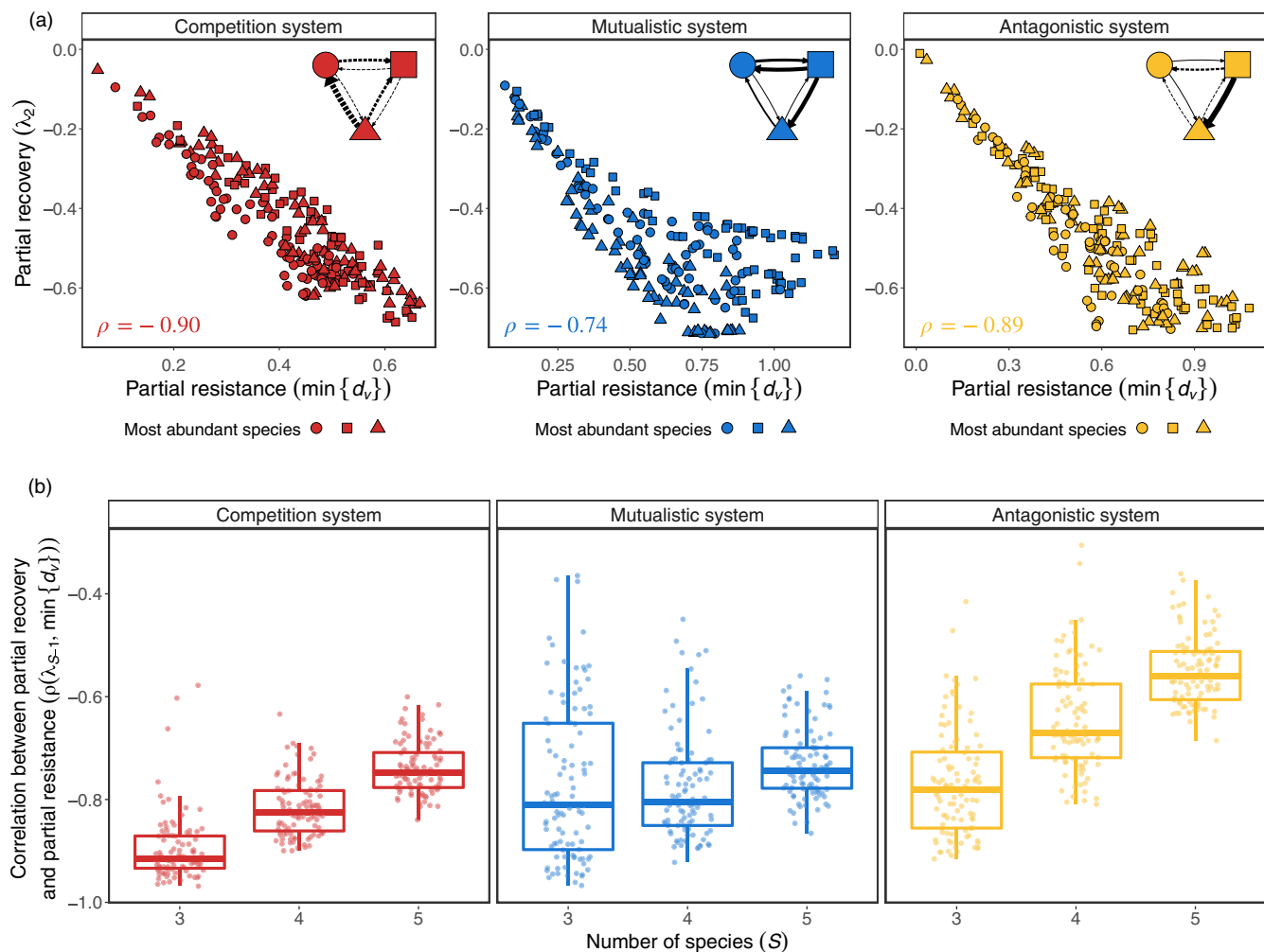


FIGURE 3 Relationship between partial recovery and partial resistance in theoretical systems. (a) Each panel shows 200 values of partial recovery (second smallest eigenvalue, λ_2) and partial resistance (distance to closest vertex, $\min\{d_v\}$) of the same illustrative theoretical random systems with three species shown in Figure 2a (red: competition system, blue: mutualistic system, and yellow: antagonistic system). Interaction networks on the top right corner of each panel depict the interaction matrices A (dashed line: negative interaction, solid line: positive interaction, and line width: interaction strength). Point shapes (circle, square and triangle) correspond to the species with the highest abundance at the equilibrium state. Correlation values between λ_2 and $\min\{d_v\}$ are shown in the bottom left corner of each panel. The competition system is the same one as shown in Figure 1. (b) Each panel shows the correlation values between λ_{S-1} and $\min\{d_v\}$ for a given type of system and for three system sizes ($S = 3, 4$ and 5). Boxplots denote the median and interquartile range and points show the actual correlation values obtained for each system type and size (100 values per boxplot corresponding to the same 100 theoretical systems from Figure 2b)

antagonistic or both interaction types) and interaction strengths (Figures S9 and S10).

Finally, we also confirmed that full resilience and partial resilience are complementary components in the experimental data. Specifically, we found that all partial correlations between recovery indicators (λ_1 and λ_2) and resistance indicators ($\min\{d_b\}$ and $\min\{d_v\}$) after controlling for the rank of the largest variable were weak in the experimental systems (Figures 4c and 5a,b). Furthermore, this complementarity was also observed in the diversity of combinations between full and partial resilience across systems. That is, while some systems appear to exhibit high relative full resilience and high relative partial resilience (i.e. relative values close to 1), others appear to exhibit low relative values (i.e. relative values close to 0; Figure 5c,d). In addition, some systems appear to exhibit

an asymmetry between the indicators—i.e. high relative full resilience and low relative partial resilience and vice versa (Figure 5c,d). Note that correlations between full recovery and full resistance ($\rho(\lambda_1, \min\{d_b\})$) as well as between partial recovery and partial resistance ($\rho(\lambda_2, \min\{d_v\})$) are strong and negative, but not perfectly correlated (Figure 4c). Therefore, we should expect a strong qualitative mapping, but not a perfect quantitative match between the position of a system in Figure 5c and its position in Figure 5d. This is confirmed by strong and positive correlations between relative full recovery and relative full resistance ($\rho(\lambda_1, \min\{d_b\}) = 0.83$) as well as between relative partial recovery and relative partial resistance ($\rho(\lambda_2, \min\{d_v\}) = 0.64$). In sum, our results reveal that a wide diversity of relationships between full and partial resilience is possible across ecological systems.

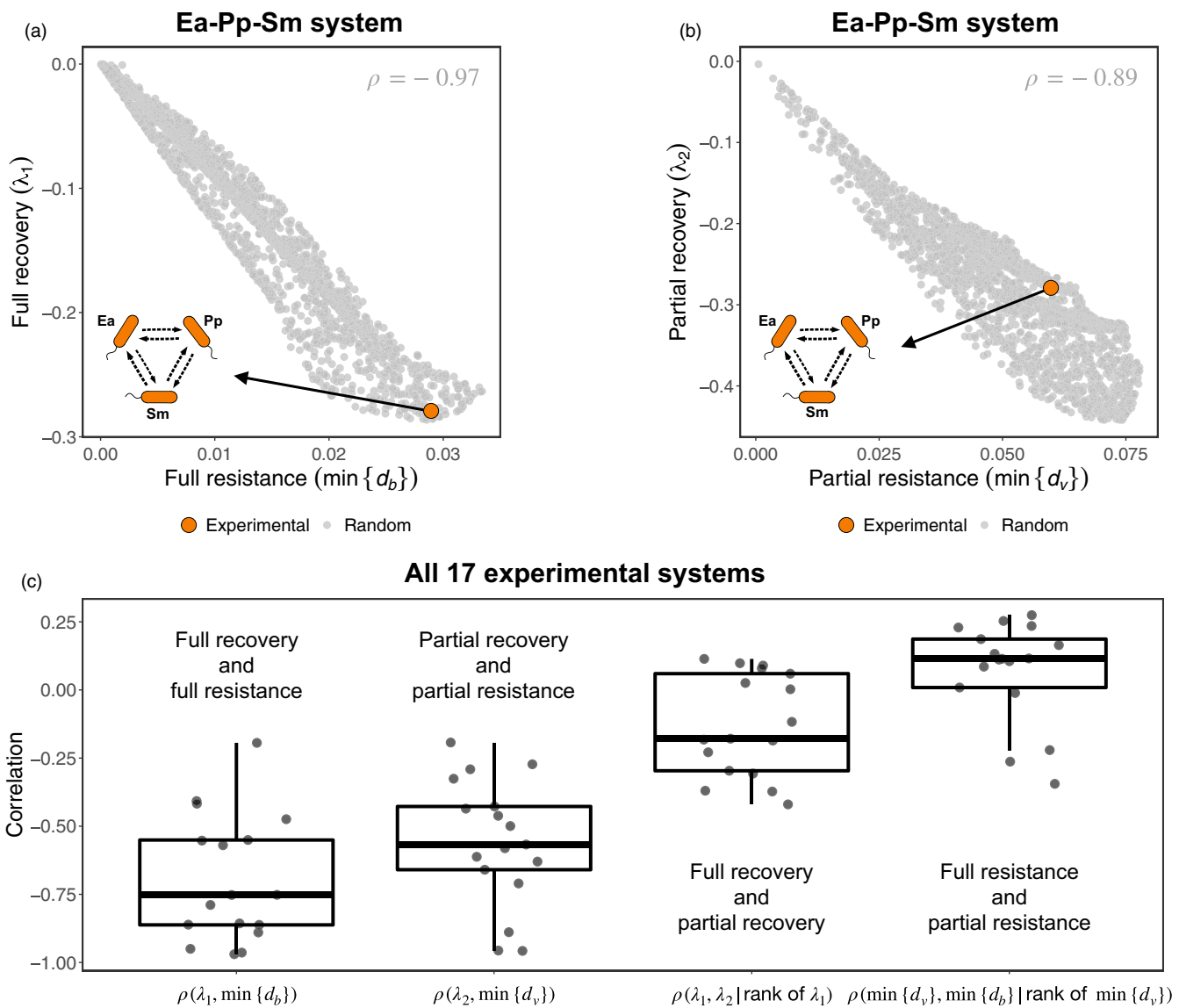


FIGURE 4 Relationship between recovery and resistance in experimental microbial systems. (a) Full recovery (largest eigenvalue, λ_1) and full resistance (distance to closest border, $\min\{d_b\}$) for one illustrative 3-species experimental system. Each grey point corresponds to one of 2,000 randomly sampled feasible and dynamically stable equilibrium states \mathbf{N}^* and the orange point corresponds to the λ_1 and $\min\{d_b\}$ values of the experimentally parameterized system. (b) Partial recovery (second smallest eigenvalue, λ_2) and partial resistance (distance to closest vertex, $\min\{d_v\}$) for the same experimental system shown in (a). In (a) and (b), the interaction network depicts the competition interactions between *Enterobacter aerogenes* (Ea), *Pseudomonas putida* (Pp) and *Serratia marcescens* (Sm). Correlation values computed using the grey points are shown in the top right corner of each panel. (c) Each boxplot shows a given correlation computed for all 17 experimental systems. Note that $\rho(\lambda_1, \min\{d_b\})$ and $\rho(\lambda_2, \min\{d_v\})$ are expected to be strong and negative, while $\rho(\lambda_1, \lambda_2 | \text{rank of } \lambda_1)$ and $\rho(\min\{d_v\}, \min\{d_b\} | \text{rank of } \min\{d_v\})$ are expected to be close to zero. Boxplots denote the median and interquartile range and points show the actual correlation values obtained for each system (17 values per boxplot corresponding to the 17 experimental systems)

4 | DISCUSSION

The resilience of ecological systems to perturbations is one of the most important yet broadly defined concepts in ecology and sustainability science (Folke et al., 2016; Hodgson et al., 2015; Pimm et al., 2019). Recently, the definition of resilience in ecology has been converging to the capacity of an ecological system to resist and recover from external perturbations (Capdevila et al., 2020; Hodgson et al., 2015). However, there are still many open questions about how to measure

the response of multispecies systems to different types of perturbation, and the extent to which these responses provide complementary information (Donohue et al., 2016; Domínguez-García et al., 2019; Kéfi et al., 2019). Understanding the different components of resilience and their interconnections with respect to different types of perturbation is paramount to implement risk assessment and conservation strategies in ecological systems (Folke et al., 2004; Folke et al., 2016).

Here, we have introduced a new perspective in order to expand the way we measure resilience and understand the connections

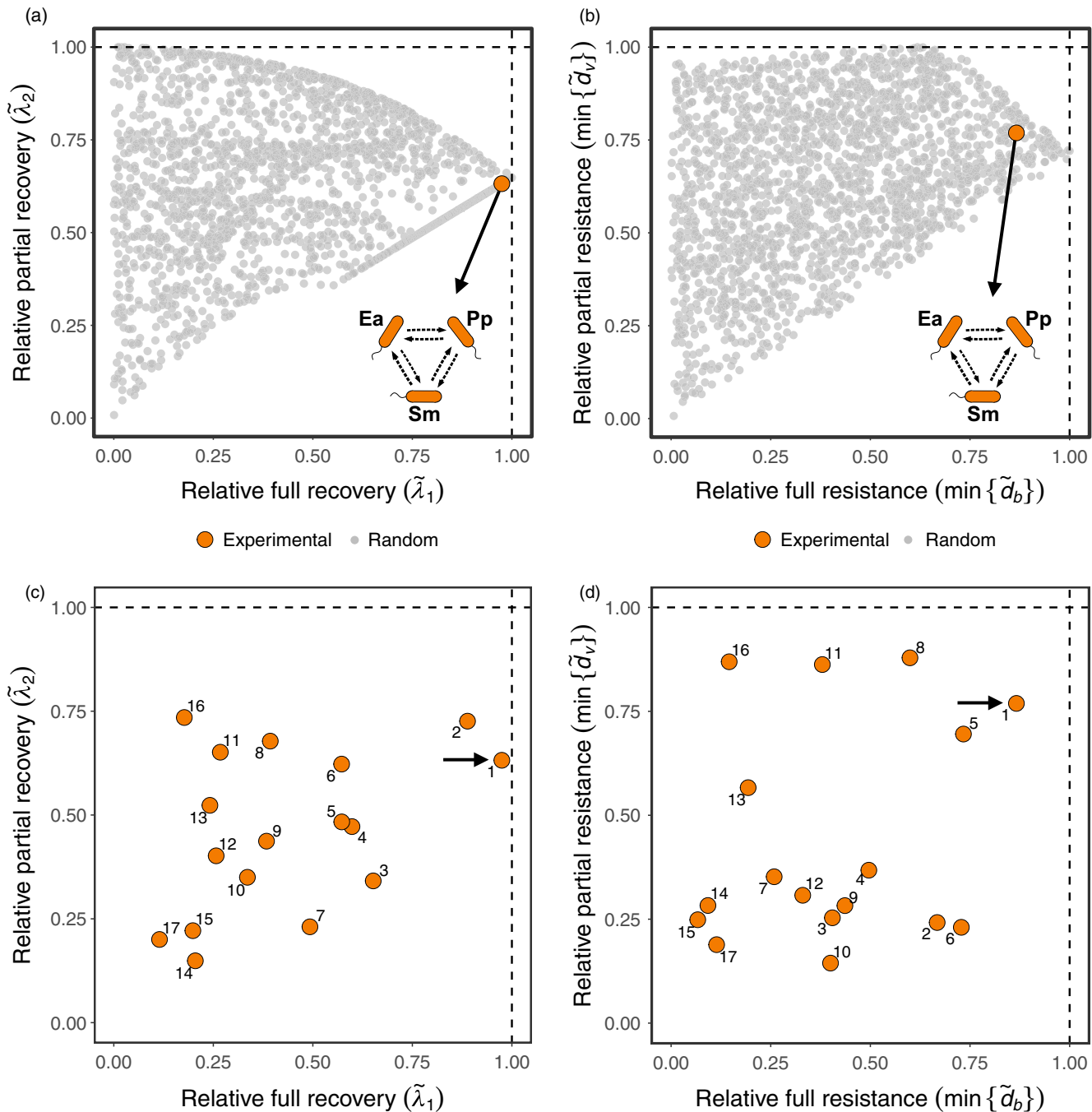


FIGURE 5 Complementarity between full and partial resilience in experimental microbial systems. (a) Relative full recovery ($\tilde{\lambda}_1$) and relative partial recovery ($\tilde{\lambda}_2$) for the same illustrative 3-species experimental system from Figure 4a (large orange point) as well as 2,000 values of $\tilde{\lambda}_1$ and $\tilde{\lambda}_2$ randomly sampled across the feasibility domain ($D_F(\mathbf{A})$) of this system (small gray points). (b) Relative full resistance ($\min\{\tilde{d}_b\}$) and relative partial resistance ($\min\{\tilde{d}_v\}$) for the same system shown in (a) (large orange point) as well as 2,000 values of $\min\{\tilde{d}_b\}$ and $\min\{\tilde{d}_v\}$ randomly sampled across $D_F(\mathbf{A})$ (small gray points). In (a) and (b), the interaction network depicts the competition interactions between *Enterobacter aerogenes* (Ea), *Pseudomonas putida* (Pp) and *Serratia marcescens* (Sm). Note that systems close to 1 (dashed lines) are maximizing recovery and/or resistance. (c) Relative full ($\tilde{\lambda}_1$) and partial ($\tilde{\lambda}_2$) recovery for all 17 experimentally parameterized 3-species systems. The point highlighted with an arrow represents the system depicted in (a) and labels next to points indicate the experimental systems (Table S3). (d) Relative full ($\min\{\tilde{d}_b\}$) and partial ($\min\{\tilde{d}_v\}$) resistance for the same 17 experimentally parameterized 3-species systems shown in (c). The point highlighted with an arrow represents the system depicted in (b) and labels correspond to the same systems as in (c).

among its components in three major ways. First, by acknowledging that external perturbations can be of any type (i.e. abundance or parameter perturbations), we have extended and integrated dynamical

(i.e. focused on abundance perturbations) and structural (i.e. focused on parameter perturbations) indicators of resilience (Arnoldi & Haegeman, 2016; Cenci & Saavedra, 2018; Saavedra et al., 2017).

Specifically, we have found a clear link between a dynamical stability indicator (long-term return rate of a system to a dynamically stable equilibrium after small abundance perturbations) and a structural stability indicator (the largest random parameter perturbation that a system can withstand before losing species). Thus, differently from previous studies that have analysed the associations between several resilience indicators (Domínguez-García et al., 2019; Hillebrand et al., 2018), here we have focused only on recovery and resistance and suggest a fundamental mathematical link between them when the dynamics follows the LV model. This suggests that other potential mathematical links may exist between frequently used dynamical and structural indicators of resilience (Arnoldi et al., 2016; Domínguez-García et al., 2019).

Second, we have found that recovery and resistance are interconnected when focusing on either full or partial components. We have defined full resilience as the capacity of a system to maintain its full species composition through the recovery and resistance of all species. In turn, we have defined partial resilience as the capacity of a system to maintain a partial species composition through the recovery and resistance of a subset of species. Specifically, we have shown that, under the LV model, fast (full or partial) recovery from abundance perturbations implies a high (full or partial) resistance to parameter perturbations. Therefore, we hypothesize that other hidden connections between resilience indicators may be found if analysed through the lens of full and partial components (Kéfi et al., 2019). From a practical point of view, this connection between recovery and resistance means that we can monitor both of these aspects of resilience using a small number of indicators (e.g. the eigenvalues of the Jacobian matrix of a system).

Third, we have found that full and partial resilience (either recovery or resistance) can be treated as complementary components. Thus, our study proposes a novel way to understand orthogonal dimensions of ecological resilience (Domínguez-García et al., 2019; Hillebrand et al., 2018). Interestingly, full resilience is related to individual risk, whereas partial resilience is related to systemic risk, two important concepts in ecological, financial and other complex systems (Beale et al., 2011; Levin, 1998). In fact, because full and partial resilience are complementary, focusing on only one of these components may provide a misleading risk assessment of ecological systems (Beale et al., 2011). For example, our results show that a system that minimizes systemic risk (i.e. is located as far as possible from the vertices of the feasibility domain) may still have a high risk of losing individual species (i.e. is located close to a border of the feasibility domain; Figure 1c,d). In particular, the existence of a wide diversity of relationships between full and partial resilience in the studied experimental microbial systems suggests that future work may investigate the extent to which these systems may be more exposed to individual or systemic risk in the face of perturbations.

Our theoretical results can in principle be validated by performing perturbation experiments with simple experimental systems (e.g. microbial systems). For instance, one can measure the recovery

rate of a system after small abundance perturbations (e.g. a single removal/addition of individuals/biomass, Steiner et al., 2006) and the resistance to extinctions after structural perturbations (e.g. a fixed change in temperature, Tabi et al., 2020 or resource availability, Hoek et al., 2016) over a set of baseline environmental conditions. Then, one can measure the association between dynamical and structural indicators, that is, recovery rate and resistance to extinctions. Furthermore, both indicators can be divided into their full (e.g. abundances fully recover, no single-species extinctions) and partial (e.g. abundances partially recover, no systemic collapse) components. For a given system, our theory purports an association between full (partial) recovery and full (partial) resistance (Figure 4a,b), and no particular association between full and partial components (recovery or resistance; Figure 5a,b).

Finally, it is worth mentioning that our indicators of resilience are formally derived under the assumptions of feasible and dynamically stable equilibria with the classic LV model (Case, 2000). Thus, these assumptions have to be fulfilled in order to apply our framework using empirical data. Nevertheless, multiple methods have been developed to estimate the structure of nonequilibrium systems (e.g. Jacobian matrix) without assuming a parameterized population dynamics model (i.e. a nonparametric approach, Deyle et al., 2016; Ives et al., 2003; Ushio et al., 2018). In particular, previous work has shown that the divergence of a nonequilibrium vector field (characterized by the trace of the Jacobian matrix) is associated with the extent to which the trajectory of the system changes after parameter perturbations (Cenci et al., 2020; Cenci & Saavedra, 2019)—a measure of resistance. Thus, these previous results indicate that it may be possible to merge concepts from dynamical and structural stability also under a nonparametric approach. In this sense, we believe that our study may also add to the unification of parametric and nonparametric approaches (Song & Saavedra, 2020) and could be expanded to be used with different types of empirical data.

ACKNOWLEDGEMENTS

Funding to S.S. was provided by NSF grant No. DEB-2024349. We thank the two reviewers and the editors for suggestions that improved our paper. The authors declare no competing financial interests.

AUTHORS' CONTRIBUTIONS

All authors designed the study; L.P.M. and C.S. performed the analysis; S.S. supervised the study. All authors wrote the manuscript.

DATA AVAILABILITY STATEMENT

The R code and data supporting the results are archived at <https://doi.org/10.5281/zenodo.4390874> (MITEcology, 2020).

ORCID

Lucas P. Medeiros  <https://orcid.org/0000-0002-0320-5058>

Chuliang Song  <https://orcid.org/0000-0001-7490-8626>

Serguei Saavedra  <https://orcid.org/0000-0003-1768-363X>

REFERENCES

- Allesina, S., & Tang, S. (2012). Stability criteria for complex ecosystems. *Nature*, 483(7388), 205–208. <https://doi.org/10.1038/nature10832>
- Arnold, V. I. (1988) *Geometrical methods in the theory of ordinary differential equations* (2nd ed.). Springer.
- Arnoldi, J. F., & Haegeman, B. (2016). Unifying dynamical and structural stability of equilibria. *Proceedings of the Royal Society A: Mathematical, Physical and Engineering Sciences*, 472(2193), 20150874–<https://doi.org/10.1098/rspa.2015.0874>
- Arnoldi, J. F., Loreau, M., & Haegeman, B. (2016). Resilience, reactivity and variability: A mathematical comparison of ecological stability measures. *Journal of Theoretical Biology*, 389, 47–59. <https://doi.org/10.1016/j.jtbi.2015.10.012>
- Barabás, G., Michalska-Smith, M. J., & Allesina, S. (2017). Self-regulation and the stability of large ecological networks. *Nature Ecology and Evolution*, 1, 1870–1875. <https://doi.org/10.1038/s41559-017-0357-6>
- Beale, N., Rand, D. G., Battey, H., Croxton, K., May, R. M., & Nowak, M. A. (2011). Individual versus systemic risk and the regulator's dilemma. *Proceedings of the National Academy of Sciences of the United States of America*, 108, 12647–12652. <https://doi.org/10.1073/pnas.1105882108>
- Burkle, L. A., Marlin, J. C., & Knight, T. M. (2013). Plant-pollinator interactions over 120 years: Loss of species, co-occurrence, and function. *Science*, 339, 1611–1615. <https://doi.org/10.1126/science.1232728>
- Capdevila, P., Stott, I., Beger, M., & Salguero-Gómez, R. (2020). Towards a comparative framework of demographic resilience. *Trends in Ecology & Evolution*. <https://doi.org/10.1016/j.tree.2020.05.001>
- Carpenter, S. R., Kraft, C. E., Wright, R., He, X., Soranno, P. A., & Hodgson, J. R. (1992). Resilience and resistance of a lake phosphorus cycle before and after food web manipulation. *The American Naturalist*, 140, 781–798. <https://doi.org/10.1086/285440>
- Case, T. J. (2000). *An illustrated guide to theoretical ecology*. Oxford University Press.
- Cenci, S., Medeiros, L. P., Sugihara, G., & Saavedra, S. (2020). Assessing the predictability of nonlinear dynamics under smooth parameter changes. *Journal of the Royal Society Interface*, 17, 20190627. <https://doi.org/10.1098/rsif.2019.0627>
- Cenci, S., & Saavedra, S. (2018). Structural stability of nonlinear population dynamics. *Physical Review E*, 97. <https://doi.org/10.1103/PhysRevE.97.012401>
- Cenci, S., & Saavedra, S. (2019). Non-parametric estimation of the structural stability of non-equilibrium community dynamics. *Nature Ecology and Evolution*, 3, 912. <https://doi.org/10.1038/s41559-019-0879-1>
- Constable, G. W. A., & McKane, A. J. (2015). Models of genetic drift as limiting forms of the Lotka-Volterra competition model. *Physical Review Letters*, 114. <https://doi.org/10.1103/PhysRevLett.114.038101>
- Costello, E. K., Stagaman, K., Dethlefsen, L., Bohannan, B. J., & Relman, D. A. (2012). The application of ecological theory toward an understanding of the human microbiome. *Science*, 336, 1255–1262. <https://doi.org/10.1126/science.1224203>
- Coulson, T., Kendall, B. E., Bartholdi, J., Plard, F., Schindler, S., Ozgul, A., & Gaillard, J. M. (2017). Modeling adaptive and nonadaptive responses of populations to environmental change. *The American Naturalist*, 190, 313–336. <https://doi.org/10.1086/692542>
- Dakos, V., Carpenter, S. R., van Nes, E. H., & Scheffer, M. (2015). Resilience indicators: Prospects and limitations for early warnings of regime shifts. *Philosophical Transactions of the Royal Society B: Biological Sciences*, 370, 20130263.
- Deyle, E. R., May, R. M., Munch, S. B., & Sugihara, G. (2016). Tracking and forecasting ecosystem interactions in real time. *Proceedings of the Royal Society B: Biological Sciences*, 283, 20152258. <https://doi.org/10.1098/rspb.2015.2258>
- Dobrinevski, A., & Frey, E. (2012). Extinction in neutrally stable stochastic Lotka-Volterra models. *Physical Review E*, 85. <https://doi.org/10.1103/PhysRevE.85.051903>
- Domínguez-García, V., Dakos, V., & Kéfi, S. (2019). Unveiling dimensions of stability in complex ecological networks. *Proceedings of the National Academy of Sciences of the United States of America*, 116, 25714–25720. <https://doi.org/10.1073/pnas.1904470116>
- Donohue, I., Hillebrand, H., Montoya, J. M., Petchey, O. L., Pimm, S. L., Fowler, M. S., Healy, K., Jackson, A. L., Lurgi, M., McClean, D., O'Connor, N. E., O'Gorman, E. J., & Yang, Q. (2016). Navigating the complexity of ecological stability. *Ecology Letters*, 19, 1172–1185. <https://doi.org/10.1111/ele.12648>
- Dougoud, M., Vinckenbosch, L., Rohr, R. P., Bersier, L. F., & Mazza, C. (2018). The feasibility of equilibria in large ecosystems: A primary but neglected concept in the complexity-stability debate. *PLOS Computational Biology*, 14, e1005988s.
- Duan, J. (2015). *An introduction to stochastic dynamics* (Vol. 51). Cambridge University Press.
- Folke, C., Biggs, R., Norström, A. V., Reyers, B., & Rockström, J. (2016). Social-ecological resilience and biosphere-based sustainability science. *Ecology and Society*, 21(3). <https://doi.org/10.5751/ES-08748-210341>
- Folke, C., Carpenter, S., Walker, B., Scheffer, M., Elmqvist, T., Gunderson, L., & Holling, C. S. (2004). Regime shifts, resilience, and biodiversity in ecosystem management. *Annual Review of Ecology, Evolution, and Systematics*, 35. <https://doi.org/10.1146/annurev.ecolsys.35.021103.105711>
- Friedman, J., Higgins, L. M., & Gore, J. (2017). Community structure follows simple assembly rules in microbial microcosms. *Nature Ecology and Evolution*, 1. <https://doi.org/10.1038/s41559-017-0109>
- Gibbs, H. L., & Grant, P. R. (1987). Ecological consequences of an exceptionally strong el niño event on Darwin's finches. *Ecology*, 68, 1735–1746.
- Grilli, J., Adorisio, M., Suweis, S., Barabás, G., Banavar, J. R., Allesina, S., & Maritan, A. (2017). Feasibility and coexistence of large ecological communities. *Nature Communications*, 8, 14389. <https://doi.org/10.1038/ncomms14389>
- Hillebrand, H., Langenheder, S., Lebret, K., Lindström, E., Östman, Ö., & Striebel, M. (2018). Decomposing multiple dimensions of stability in global change experiments. *Ecology Letters*, 21, 21–30. <https://doi.org/10.1111/ele.12867>
- Hodgson, D., McDonald, J. L., & Hosken, D. J. (2015). What do you mean, 'resilient'? *Trends in Ecology & Evolution*, 30, 503–506. <https://doi.org/10.1016/j.tree.2015.06.010>
- Hoek, T. A., Axelrod, K., Biancalani, T., Yurtsev, E. A., Liu, J., & Gore, J. (2016). Resource availability modulates the cooperative and competitive nature of a microbial cross-feeding mutualism. *PLoS Biology*, 14, e1002540. <https://doi.org/10.1371/journal.pbio.1002540>
- Hofbauer, J., & Sigmund, K. (1998). *Evolutionary games and population dynamics*. Cambridge University Press.
- Ives, A. R., Dennis, B., Cottingham, K., & Carpenter, S. (2003). Estimating community stability and ecological interactions from time-series data. *Ecological Monographs*, 73, 301–330.
- Justus, J. (2013). Philosophical issues in ecology. In K. Kampourakis (Ed.), *The philosophy of biology* (pp. 343–371). Springer.
- Kéfi, S., Domínguez-García, V., Donohue, I., Fontaine, C., Thébaud, E., & Dakos, V. (2019). Advancing our understanding of ecological stability. *Ecology Letters*, 22, 1349–1356. <https://doi.org/10.1111/ele.13340>
- Levin, S. A. (1998). Ecosystems and the biosphere as complex adaptive systems. *Ecosystems*, 1, 431–436. <https://doi.org/10.1007/s100219900037>
- Logofet, D. (2018). *Matrices and graphs stability problems in mathematical ecology*. CRC Press.
- May, R. M. (1972). Will a large complex system be stable? *Nature*, 238, 413–414. <https://doi.org/10.1038/238413a0>
- Medeiros, L. P., Boege, K., del Val, E., Zaldivar-Riverón, A., & Saavedra, S. (2021). Observed ecological communities are formed by species combinations that are among the most likely to persist under

- changing environments. *The American Naturalist*, 197(1), <https://doi.org/10.1086/711663>
- MITEcology. (2020). Data from: MITEcology/JAE_Medeiros_etal_2021_v1.0. <https://doi.org/10.5281/zenodo.4390874>
- Murdoch, W., Briggs, C., & Nisbet, R. (2003). *Consumer-resource dynamics*. Princeton University Press.
- Novak, M., Yeakel, J. D., Noble, A. E., Doak, D. F., Emmerson, M., Estes, J. A., Jacob, U., Tinker, M. T., & Wootton, J. T. (2016). Characterizing species interactions to understand press perturbations: What is the community matrix? *Annual Review of Ecology, Evolution, and Systematics*, 47. <https://doi.org/10.1146/annurev-ecolsys-032416-010215>
- Pimm, S. L., Donohue, I., Montoya, J. M., & Loreau, M. (2019). Measuring resilience is essential to understand it. *Nature Sustainability*, 2, 895–897. <https://doi.org/10.1038/s41893-019-0399-7>
- Pimm, S., & Lawton, J. (1977). Number of trophic levels in ecological communities. *Nature*, 268, 329–331. <https://doi.org/10.1038/268329a0>
- Rohr, R. P., Saavedra, S., Peralta, G., Frost, C. M., Bersier, L. F., Bascompte, J., & Tylianakis, J. M. (2016). Persist or produce: A community trade-off tuned by species evenness. *The American Naturalist*, 188, 411–422. <https://doi.org/10.1086/688046>
- Saavedra, S., Medeiros, L. P., & AlAdwani, M. (2020). Structural forecasting of species persistence under changing environments. *Ecology Letters*, 23, 1511–1521. <https://doi.org/10.1111/ele.13582>
- Saavedra, S., Rohr, R. P., Bascompte, J., Godoy, O., Kraft, N. J. B., & Levine, J. M. (2017). A structural approach for understanding multi-species coexistence. *Ecological Monographs*, 87, 470–486. <https://doi.org/10.1002/ecm.1263>
- Smale, S. (1967). Differentiable dynamical systems. *Bulletin of the American Mathematical Society*, 73, 747–817.
- Song, C., Ahn, S. V., Rohr, R. P., & Saavedra, S. (2020). Towards a probabilistic understanding about the context-dependency of species interactions. *Trends in Ecology & Evolution*, 35, 384–396. <https://doi.org/10.1016/j.tree.2019.12.011>
- Song, C., Rohr, R. P., & Saavedra, S. (2018). A guideline to study the feasibility domain of multitrophic and changing ecological communities. *Journal of Theoretical Biology*, 450, 30–36. <https://doi.org/10.1016/j.jtbi.2018.04.030>
- Song, C., & Saavedra, S. (2018). Will a small randomly-assembled community be feasible and stable. *Ecology*, 99, 743–751. <https://doi.org/10.1002/ecy.2125>
- Song, C., & Saavedra, S. (2020). Bridging parametric and nonparametric measures of species interactions unveils new insights of non-equilibrium dynamics. *BioRxiv*.
- Steiner, C. F., Long, Z. T., Krumins, J. A., & Morin, P. J. (2006). Population and community resilience in multitrophic communities. *Ecology*, 87, 996–1007.
- Strogatz, S. H. (1994). *Nonlinear dynamics and Chaos: With applications to physics, biology, chemistry, and engineering*. Addison-Wesley Pub.
- Tabi, A., Pennekamp, F., Altermatt, F., Alther, R., Fronhofer, E. A., Horgan, K., Mächler, E., Pontarp, M., Petchey, O. L., & Saavedra, S. (2020). Species multidimensional effects explain idiosyncratic responses of communities to environmental change. *Nature Ecology and Evolution*, 4, 1036–1043. <https://doi.org/10.1038/s41559-020-1206-6>
- Ushio, M., Hsieh, C. H., Masuda, R., Deyle, E. R., Ye, H., Chang, C. W., Sugihara, G., & Kondoh, M. (2018). Fluctuating interaction network and time-varying stability of a natural fish community. *Nature*, 554, 360–363. <https://doi.org/10.1038/nature25504>

SUPPORTING INFORMATION

Additional supporting information may be found online in the Supporting Information section.

How to cite this article: Medeiros LP, Song C, Saavedra S. Merging dynamical and structural indicators to measure resilience in multispecies systems. *J Anim Ecol*. 2021;00:1–14. <https://doi.org/10.1111/1365-2656.13421>

Supplementary Information

Merging dynamical and structural indicators to measure resilience in
multispecies systems

Lucas P. Medeiros^{1*}, Chuliang Song^{1,2,3*}, Serguei Saavedra^{1†}

¹Department of Civil and Environmental Engineering, MIT,
77 Massachusetts Av., 02139 Cambridge, MA, USA

²Department of Biology, Quebec Centre for Biodiversity Science, McGill University,
Montreal, Canada H3A 1B1

³Department of Ecology and Evolutionary Biology, University of Toronto,
25 Willcocks Street, Toronto, Ontario M5S 3B2 Canada

*Equal contribution

†To whom correspondence should be addressed. E-mail: sersaa@mit.edu ORCID 0000-0003-1768-363X

	r_i
Ea	0.46
Pa	0.55
Pch	0.18
Pci	0.16
Pf	0.25
Pp	0.65
Pv	0.57
Sm	0.34

Table S1: Experimentally parameterized growth rates r_i from Friedman *et al.* (2017). Note that the parameterization follows the r-formalism (Equation (1) in the main text). Species names: *Enterobacter aerogenes* (Ea), *Pseudomonas aurantiaca* (Pa), *Pseudomonas chlororaphis* (Pch), *Pseudomonas citronellolis* (Pci), *Pseudomonas fluorescens* (Pf), *Pseudomonas putida* (Pp), *Pseudomonas veronii* (Pv), and *Serratia marcescens* (Sm).

	Ea	Pa	Pch	Pci	Pf	Pp	Pv	Sm
Ea	-3.54	-2.44	-3.86	-1.95	-5.41	-2.90	-3.86	-2.55
Pa	1.41	-7.86	-19.17	20.27	-8.88	-3.38	-0.08	-1.65
Pch	0.18	1.31	-1.64	25.77	-0.47	0.07	0.08	0.05
Pci	5.12	-0.00	-2.88	-16.00	54.24	-0.00	-0.80	4.80
Pf	0.10	-1.40	-6.00	-4.15	-5.00	-0.05	-0.35	0.50
Pp	-4.04	-7.34	-5.76	-1.11	-4.64	-4.64	-4.69	-3.90
Pv	-4.30	-1.45	-2.44	-0.00	0.10	-4.09	-5.18	-3.63
Sm	-2.18	-2.79	-3.22	-2.74	-2.97	-2.06	-2.22	-2.27

Table S2: Experimentally parameterized intra and interspecific interaction strengths a_{ij} from Friedman *et al.* (2017). Note that a_{ij} represents the per capita effect of species j (column) on species i (row) and the parameterization follows the r-formalism (Equation (1) in the main text). Species names are the same as in Table S1.

system	species 1	species 2	species 3
1	Ea	Pp	Sm
2	Pci	Pf	Pv
3	Ea	Pa	Pf
4	Ea	Pa	Pci
5	Pci	Pf	Pp
6	Pci	Pf	Sm
7	Pa	Pci	Pf
8	Pci	Pv	Sm
9	Pa	Pci	Pv
10	Pa	Pf	Pv
11	Pa	Pci	Sm
12	Ea	Pci	Pf
13	Ea	Pci	Pp
14	Ea	Pci	Pv
15	Pci	Pp	Sm
16	Pf	Pp	Sm
17	Pci	Pp	Pv

Table S3: Feasible and dynamically stable 3-species systems chosen from the pool of 8 species in Table S2. These systems are numbered following Figure 5 in the main text and species names are the same as in Table S1.

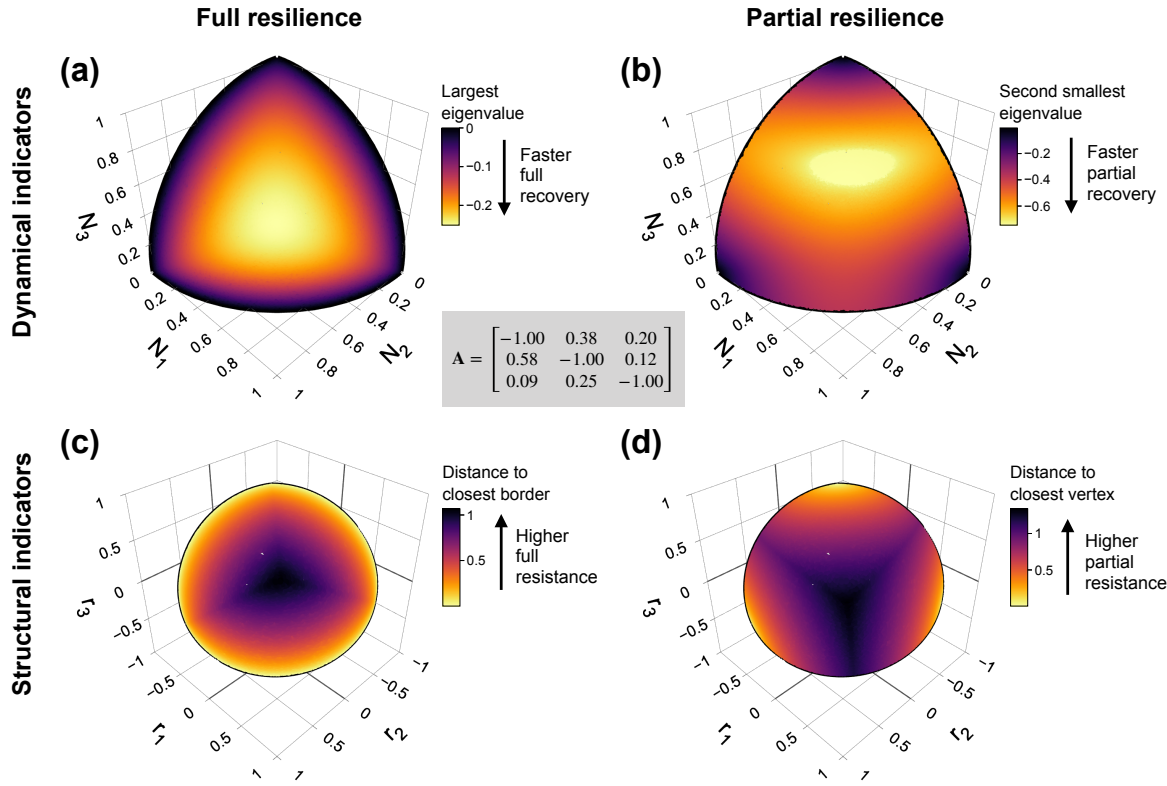


Figure S1: Dynamical and structural indicators of full and partial resilience in a mutualistic system. **(a)** An illustrative example of a 3-dimensional space of species abundances at equilibrium (\mathbf{N}^*) colored according to the largest eigenvalue of the Jacobian matrix (λ_1). The interaction matrix \mathbf{A} of this 3-species mutualistic system is shown in the center of the figure. Note that this space corresponds to the positive orthant of the unit sphere (i.e., $\|\mathbf{N}^*\| = 1$, $N_i^* > 0 \forall i$). **(b)** The same space of species abundances, but colored according to the second smallest eigenvalue of the Jacobian matrix (λ_2). **(c)** The space of intrinsic growth rates (\mathbf{r}) for the same system shown in (a) and (b) colored according to the distance to closest border ($\min\{d_b\}$) of the feasibility domain, which are indicated as black curves. Note that \mathbf{r} -vectors on the feasibility domain are normalized to unit norm (i.e., $\|\mathbf{r}\| = 1$). **(d)** The same space of intrinsic growth rates, but colored according to the distance to closest vertex ($\min\{d_v\}$) of the feasibility domain.

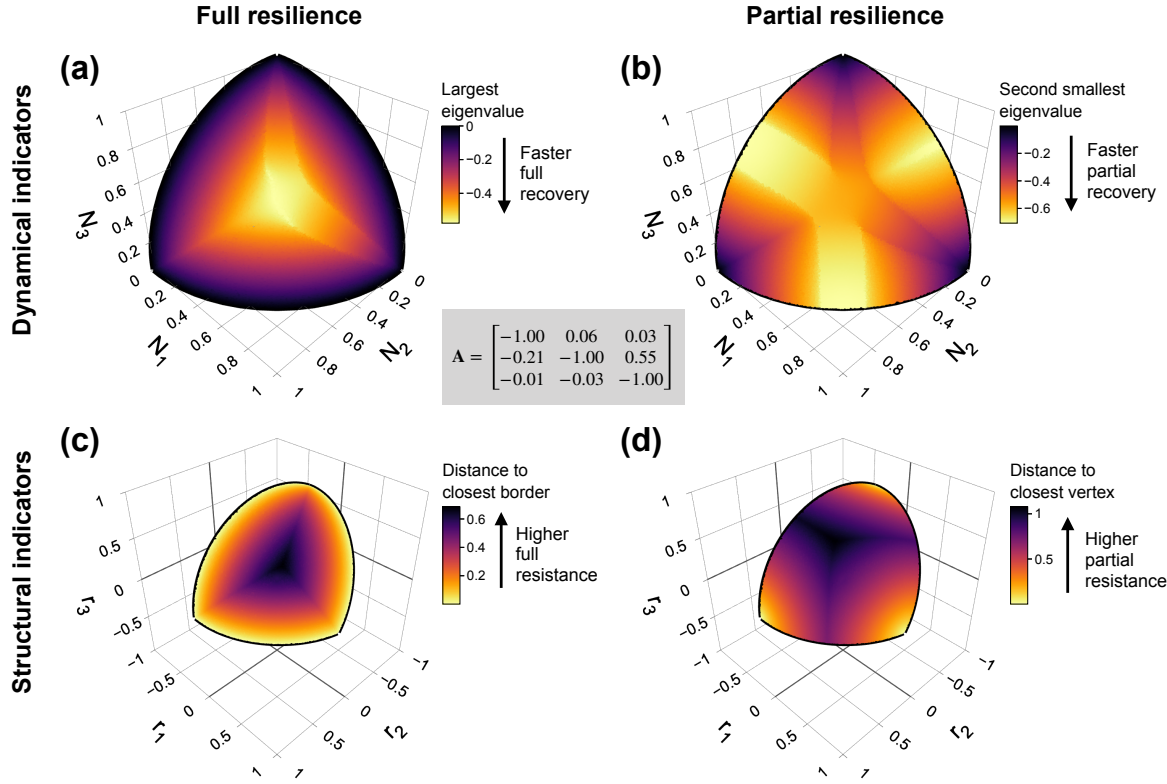


Figure S2: Dynamical and structural indicators of full and partial resilience in an antagonistic system. **(a)** An illustrative example of a 3-dimensional space of species abundances at equilibrium (\mathbf{N}^*) colored according to the largest eigenvalue of the Jacobian matrix (λ_1). The interaction matrix \mathbf{A} of this 3-species antagonistic system is shown in the center of the figure. Note that this space corresponds to the positive orthant of the unit sphere (i.e., $\|\mathbf{N}^*\| = 1, N_i^* > 0 \forall i$). **(b)** The same space of species abundances, but colored according to the second smallest eigenvalue of the Jacobian matrix (λ_2). **(c)** The space of intrinsic growth rates (\mathbf{r}) for the same system shown in (a) and (b) colored according to the distance to closest border ($\min\{d_b\}$) of the feasibility domain, which are indicated as black curves. Note that \mathbf{r} -vectors on the feasibility domain are normalized to unit norm (i.e., $\|\mathbf{r}\| = 1$). **(d)** The same space of intrinsic growth rates, but colored according to the distance to closest vertex ($\min\{d_v\}$) of the feasibility domain.

Correlation	Competition system			Mutualistic system			Antagonistic system		
	3	4	5	3	4	5	3	4	5
$\rho(\lambda_1, \min\{d_b\})$	-0.98 ± 0.01	-0.98 ± 0.01	-0.94 ± 0.02	-0.91 ± 0.07	-0.89 ± 0.06	-0.80 ± 0.09	-0.97 ± 0.02	-0.97 ± 0.02	-0.94 ± 0.01
$\rho(\lambda_{S-1}, \min\{d_v\})$	-0.90 ± 0.06	-0.82 ± 0.05	-0.74 ± 0.05	-0.77 ± 0.15	-0.78 ± 0.10	-0.74 ± 0.07	-0.77 ± 0.10	-0.65 ± 0.10	-0.55 ± 0.07

Table S4: Mean (\pm standard deviation) correlation between full recovery (largest eigenvalue, λ_1) and full resistance (distance to closest border, $\min\{d_b\}$) as well as between partial recovery (second smallest eigenvalue, λ_{S-1}) and partial resistance (distance to closest vertex, $\min\{d_v\}$). These correlation values correspond to Figures 2b and 3b from the main text. Each mean and standard deviation was computed over 100 theoretical random systems for each combination of system type (competition, mutualistic, and antagonistic system) and size ($S = 3, 4$, and 5). Note that all mean correlation values are strong and negative (≤ -0.55).

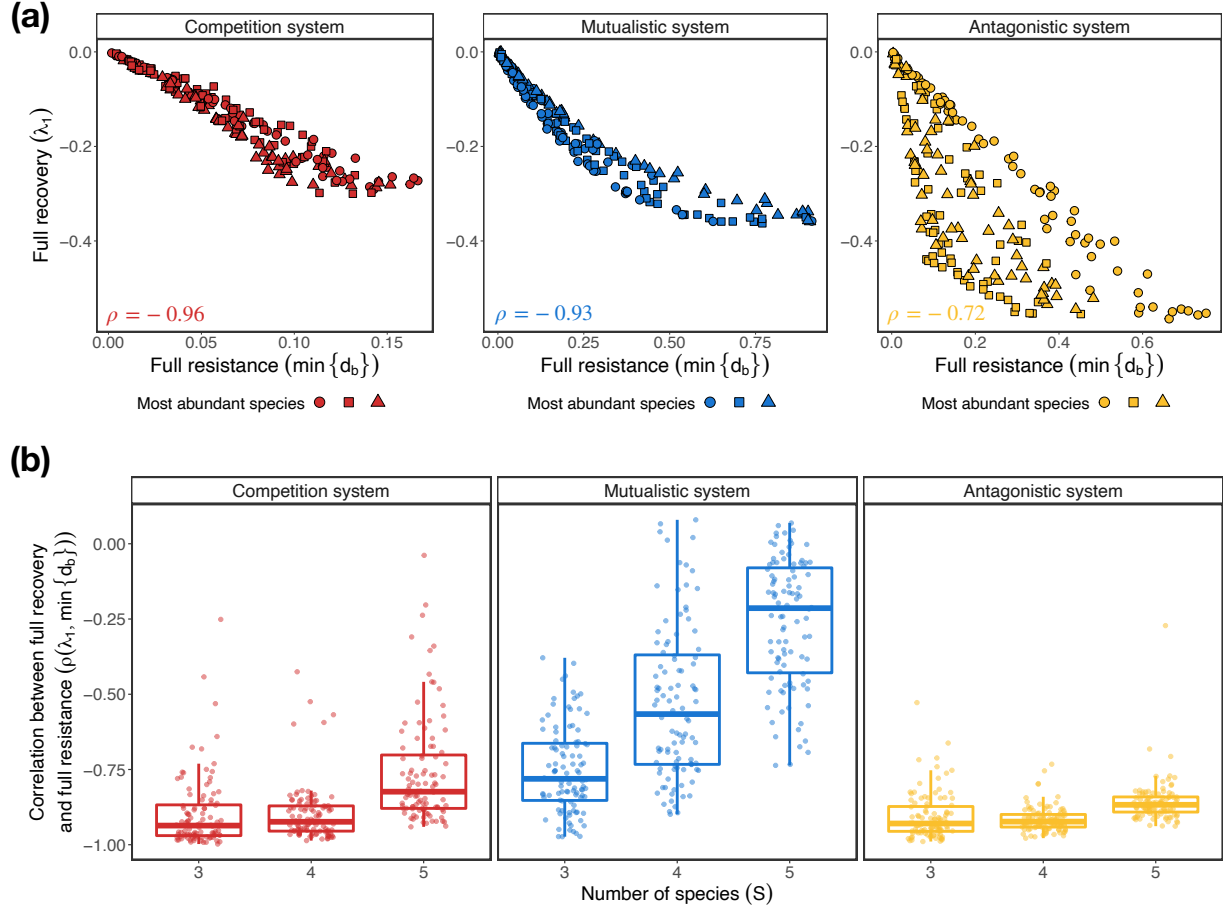


Figure S3: Relationship between full recovery and full resistance in theoretical systems with strong interspecific interactions (i.e., $\sigma^2 = \frac{1}{S}$). **(a)** Each panel shows 200 values of full recovery (largest eigenvalue, λ_1) and full resistance (distance to closest border, $\min\{d_b\}$) of one illustrative theoretical random system with three species (red: competition system, blue: mutualistic system, and yellow: antagonistic system). Point shapes (circle, square, and triangle) correspond to the species with the highest abundance at that equilibrium state. Correlation values between λ_1 and $\min\{d_b\}$ are shown in the bottom left corner of each panel. **(b)** Each panel shows the correlation values between λ_1 and $\min\{d_b\}$ for a given type of system and for three system sizes ($S = 3, 4$, and 5). Boxplots denote the median and interquartile range and points show the actual correlation values obtained for each system type and size (100 values per boxplot).

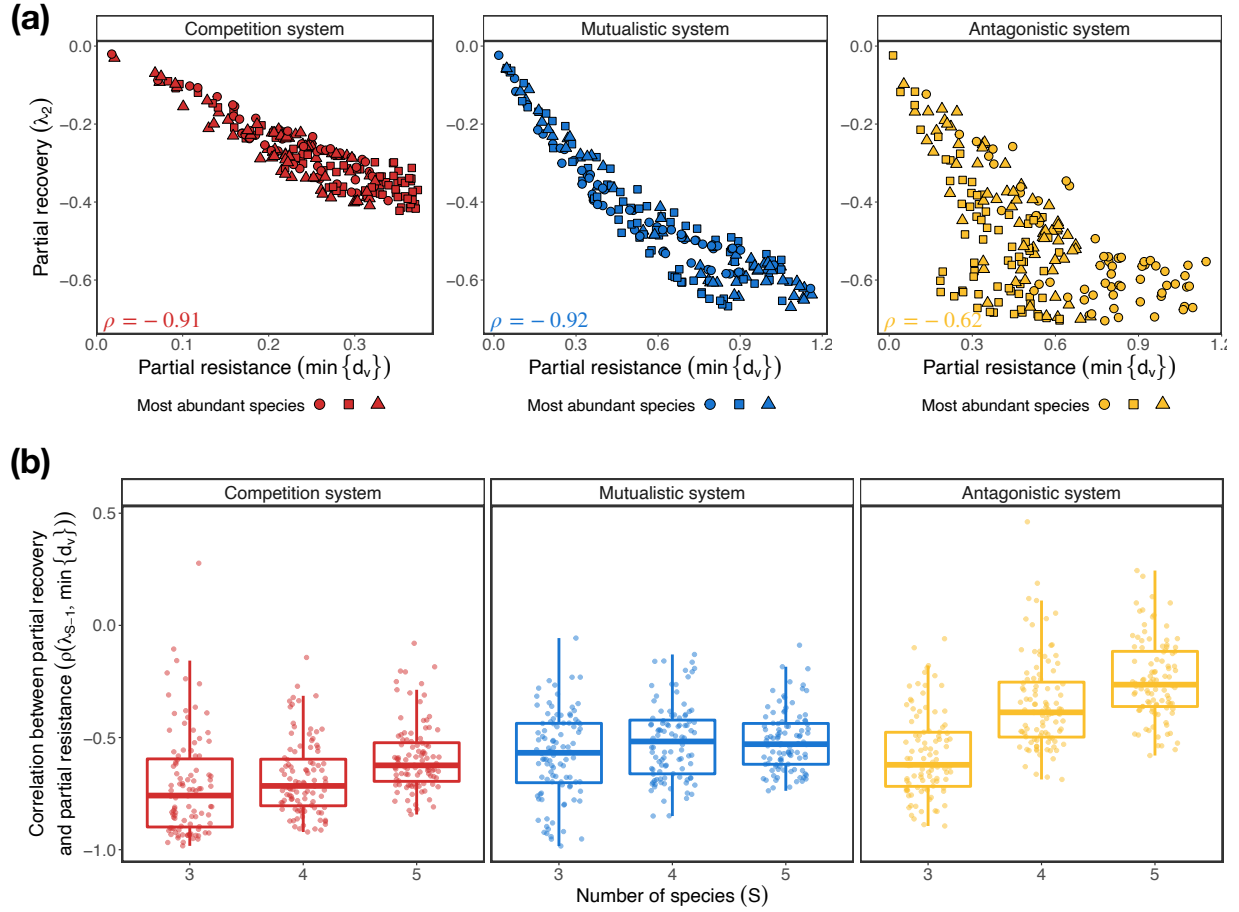


Figure S4: Relationship between partial recovery and partial resistance in theoretical systems with strong interspecific interactions (i.e., $\sigma^2 = \frac{1}{S}$). **(a)** Each panel shows 200 values of partial recovery (second smallest eigenvalue, λ_2) and partial resistance (distance to closest vertex, $\min\{d_v\}$) of the same illustrative theoretical random systems with three species shown in Figure S3 (red: competition system, blue: mutualistic system, and yellow: antagonistic system). Point shapes (circle, square, and triangle) correspond to the species with the highest abundance at the equilibrium state. Correlation values between λ_2 and $\min\{d_v\}$ are shown in the bottom left corner of each panel. **(b)** Each panel shows the correlation values between λ_{S-1} and $\min\{d_v\}$ for a given type of system and for three system sizes ($S = 3, 4$, and 5). Boxplots denote the median and interquartile range and points show the actual correlation values obtained for each system type and size (100 values per boxplot).

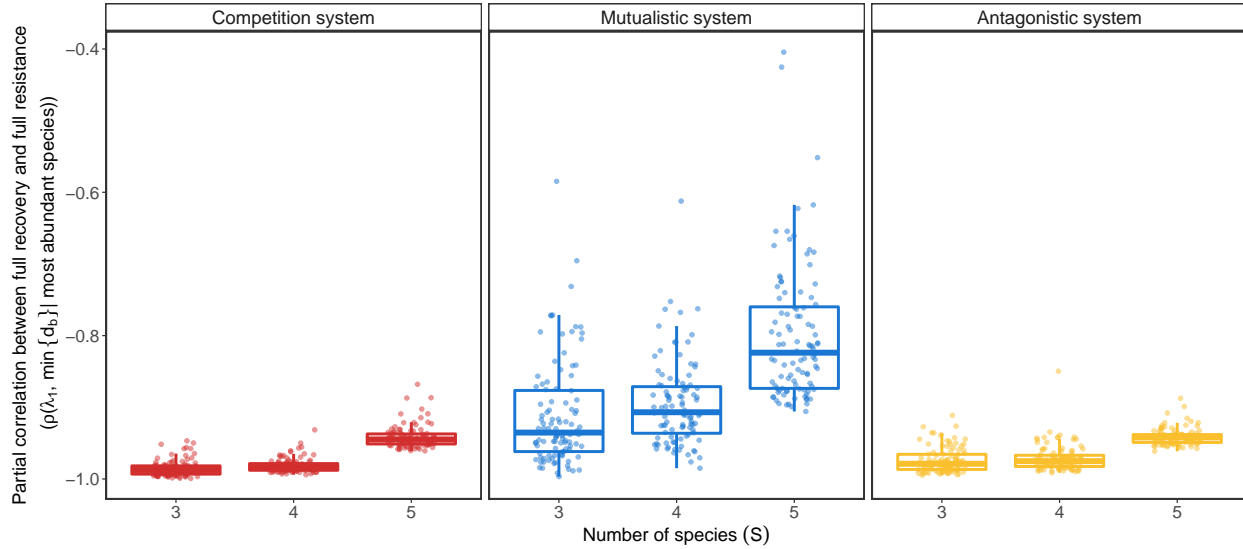


Figure S5: Partial correlation between full recovery and full resistance controlling for the most abundant species in theoretical random systems. Each panel shows the partial correlation values between full recovery (largest eigenvalue, λ_1) and full resistance (distance to closest border, $\min\{d_b\}$) while controlling for the identity of the most abundant species at equilibrium ($\rho(\lambda_1, \min\{d_b\} | \text{most abundant species})$) for a given type of system (red: competition system, blue: mutualistic system, and yellow: antagonistic system) and for three system sizes ($S = 3, 4$, and 5). Boxplots denote the median and interquartile range and points show the actual partial correlation values obtained for each system type and size (100 values per boxplot).

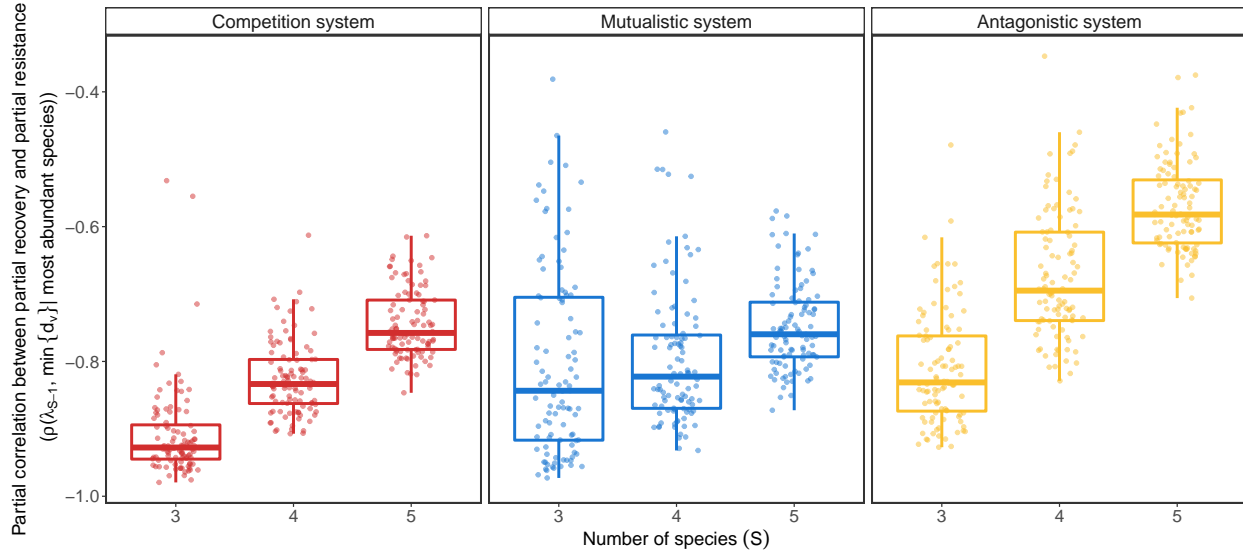


Figure S6: Partial correlation between partial recovery and partial resistance controlling for the most abundant species in theoretical random systems. Each panel shows the partial correlation values between partial recovery (second smallest eigenvalue, λ_{S-1}) and partial resistance (distance to closest vertex, $\min\{d_v\}$) while controlling for the identity of the most abundant species at equilibrium ($\rho(\lambda_{S-1}, \min\{d_v\} | \text{most abundant species})$) for a given type of system (red: competition system, blue: mutualistic system, and yellow: antagonistic system) and for three system sizes ($S = 3, 4$, and 5). Boxplots denote the median and interquartile range and points show the actual partial correlation values obtained for each system type and size (100 values per boxplot).

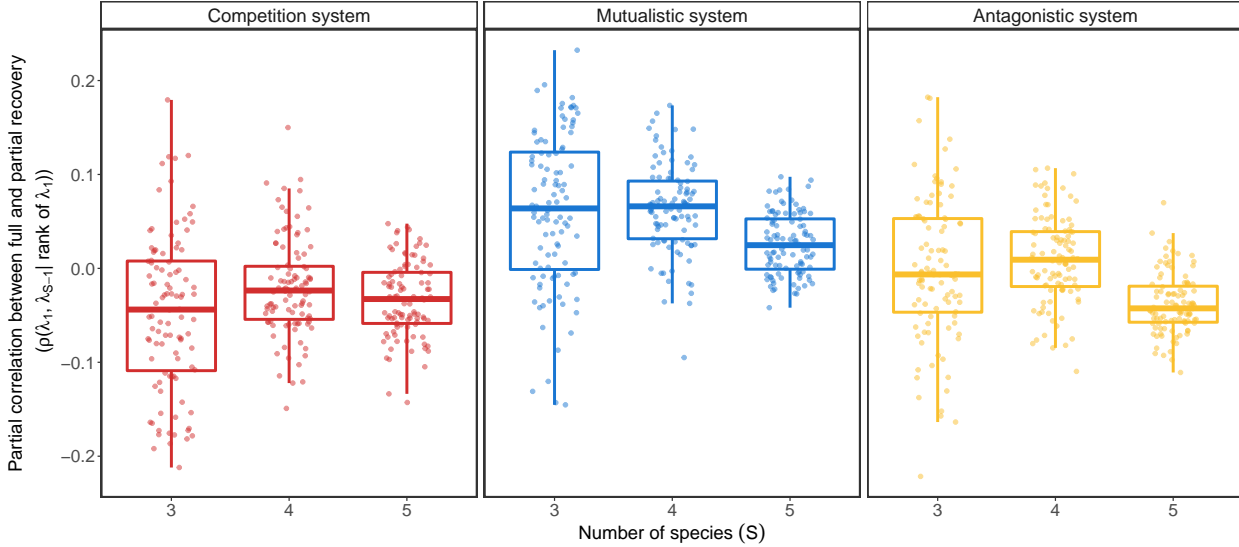


Figure S7: Partial correlation between full and partial recovery controlling for rank in theoretical random systems. Each panel shows the partial correlation values between full recovery (largest eigenvalue, λ_1) and partial recovery (second smallest eigenvalue, λ_{S-1}) while controlling for the rank of λ_1 ($\rho(\lambda_1, \lambda_{S-1} | \text{rank of } \lambda_1)$) for a given type of system (red: competition system, blue: mutualistic system, and yellow: antagonistic system) and for three system sizes ($S = 3, 4$, and 5). Note that these partial correlation values are expected to be close to zero. Boxplots denote the median and interquartile range and points show the actual partial correlation values obtained for each system type and size (100 values per boxplot).

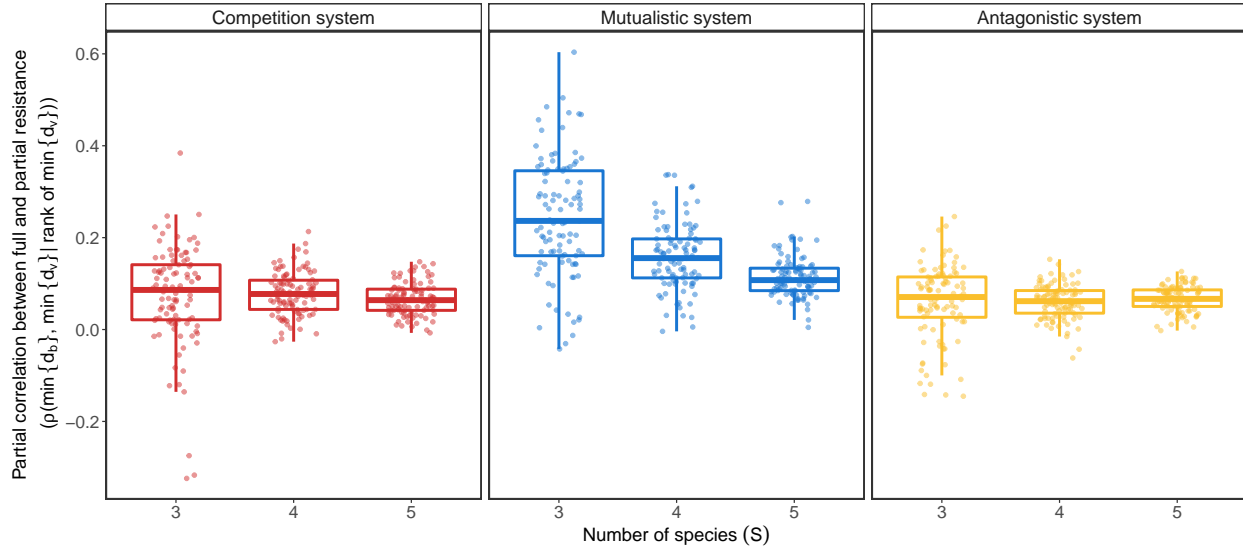


Figure S8: Partial correlation between full and partial resistance controlling for rank in theoretical random systems. Each panel shows the partial correlation values between full resistance (distance to closest border, $\min\{d_b\}$) and partial resistance (distance to closest vertex, $\min\{d_v\}$) while controlling for the rank of $\min\{d_v\}$ ($\rho(\min\{d_b\}, \min\{d_v\} | \text{rank of } \min\{d_v\})$) for a given type of system (red: competition system, blue: mutualistic system, and yellow: antagonistic system) and for three system sizes ($S = 3, 4$, and 5). Note that these partial correlation values are expected to be close to zero. Boxplots denote the median and interquartile range and points show the actual partial correlation values obtained for each system type and size (100 values per boxplot).

Partial correlation	Competition system			Mutualistic system			Antagonistic system		
	3	4	5	3	4	5	3	4	5
$\rho(\lambda_1, \min\{d_b\} \mid \text{most abundant species})$	-0.99 ± 0.01	-0.98 ± 0.01	-0.94 ± 0.02	-0.91 ± 0.07	-0.89 ± 0.06	-0.80 ± 0.09	-0.97 ± 0.02	-0.97 ± 0.02	-0.94 ± 0.01
$\rho(\lambda_{S-1}, \min\{d_v\} \mid \text{most abundant species})$	-0.91 ± 0.07	-0.82 ± 0.05	-0.74 ± 0.05	-0.80 ± 0.14	-0.80 ± 0.10	-0.75 ± 0.06	-0.81 ± 0.08	-0.67 ± 0.09	-0.57 ± 0.07
$\rho(\lambda_1, \lambda_{S-1} \mid \text{rank of } \lambda_1)$	-0.05 ± 0.08	-0.02 ± 0.05	-0.03 ± 0.04	0.06 ± 0.08	0.06 ± 0.05	0.03 ± 0.03	-0.002 ± 0.08	0.009 ± 0.05	-0.04 ± 0.03
$\rho(\min\{d_b\}, \min\{d_v\} \mid \text{rank of } \min\{d_v\})$	0.07 ± 0.11	0.08 ± 0.05	0.07 ± 0.03	0.24 ± 0.13	0.16 ± 0.07	0.11 ± 0.04	0.06 ± 0.08	0.06 ± 0.04	0.07 ± 0.03

Table S5: Mean (\pm standard deviation) partial correlations. The first and second rows show the partial correlation between full recovery (largest eigenvalue, λ_1) and full resistance (distance to closest border, $\min\{d_b\}$) as well as between partial recovery (second smallest eigenvalue, λ_{S-1}) and partial resistance (distance to closest vertex, $\min\{d_v\}$) while controlling for the identity of the most abundant species at equilibrium. Note that all mean partial correlation values in these two rows are strong and negative (≤ -0.57), similarly to Table S4. These partial correlation values correspond to Figures S5 and S6. The third and fourth rows show the partial correlation between full recovery (largest eigenvalue, λ_1) and partial recovery (second smallest eigenvalue, λ_{S-1}) as well as between full resistance (distance to closest border, $\min\{d_b\}$) and partial resistance (distance to closest vertex, $\min\{d_v\}$) while controlling for the rank of the largest variable (i.e., λ_1 or $\min\{d_v\}$). Note that most mean partial correlation values in these two rows are close to 0, showing that these indicators are complementary. These partial correlation values correspond to Figures S7 and S8. Each mean and standard deviation was computed over 100 random systems for each combination of system type (competition, mutualistic, and antagonistic system) and size ($S = 3, 4$, and 5).

Correlation	Value
$\rho(\lambda_1, \min\{d_b\})$	-0.69 ± 0.23
$\rho(\lambda_2, \min\{d_v\})$	-0.56 ± 0.23

Table S6: Mean (\pm standard deviation) correlation between full recovery (largest eigenvalue, λ_1) and full resistance (distance to closest border, $\min\{d_b\}$) as well as between partial recovery (second smallest eigenvalue, λ_2) and partial resistance (distance to closest vertex, $\min\{d_v\}$) for the 3-species experimental microbial systems. Each mean and standard deviation was computed over the 17 experimental systems. As expected, both mean correlation values are strong and negative.

Partial correlation	Value
$\rho(\lambda_1, \min\{d_b\} \mid \text{most abundant species})$	-0.70 ± 0.24
$\rho(\lambda_2, \min\{d_v\} \mid \text{most abundant species})$	-0.53 ± 0.24
$\rho(\lambda_1, \lambda_2 \mid \text{rank of } \lambda_1)$	-0.13 ± 0.19
$\rho(\min\{d_b\}, \min\{d_v\} \mid \text{rank of } \min\{d_v\})$	0.07 ± 0.18

Table S7: Mean (\pm standard deviation) partial correlations for the 3-species experimental microbial systems. The first and second rows show the partial correlation between full recovery (largest eigenvalue, λ_1) and full resistance (distance to closest border, $\min\{d_b\}$) as well as between partial recovery (second smallest eigenvalue, λ_2) and partial resistance (distance to closest vertex, $\min\{d_v\}$) while controlling for the identity of the most abundant species at equilibrium. Note that the mean partial correlation values in these two rows are strong and negative, similarly to Table S6. The third and fourth rows show the partial correlation between full recovery (largest eigenvalue, λ_1) and partial recovery (second smallest eigenvalue, λ_2) as well as between full resistance (distance to closest border, $\min\{d_b\}$) and partial resistance (distance to closest vertex, $\min\{d_v\}$) while controlling for the rank of the largest variable (i.e., λ_1 or $\min\{d_v\}$). Note that the mean partial correlation values in these two rows are close to zero, confirming the complementarity between these indicators. Each mean and standard deviation was computed over the 17 experimental systems.

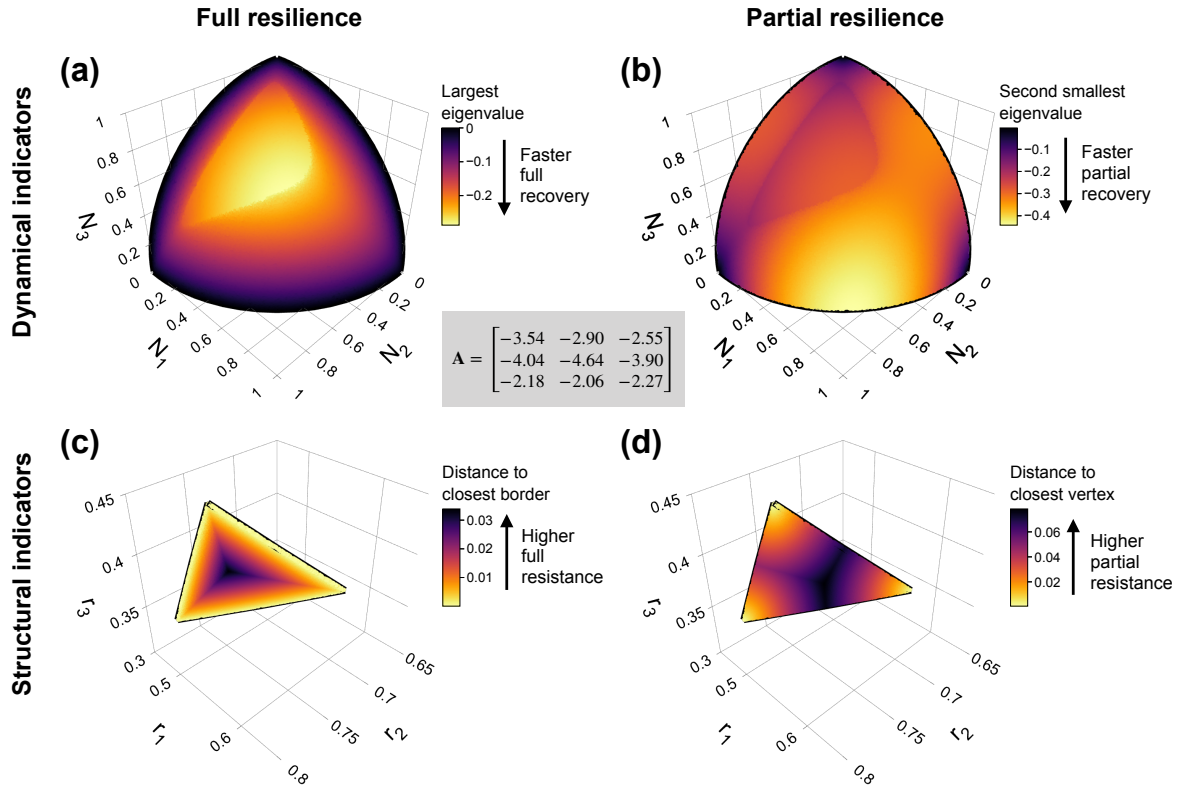


Figure S9: Dynamical and structural indicators of full and partial resilience in a competition microbial system (system 1: Ea-Pp-Sm; Tables S1 and S3). **(a)** The 3-dimensional space of species abundances at equilibrium (\mathbf{N}^*) colored according to the largest eigenvalue of the Jacobian matrix (λ_1). The interaction matrix \mathbf{A} of this 3-species system is shown in the center of the figure. Note that this space corresponds to the positive orthant of the unit sphere (i.e., $\|\mathbf{N}^*\| = 1$, $N_i^* > 0 \forall i$). **(b)** The same space of species abundances, but colored according to the second smallest eigenvalue of the Jacobian matrix (λ_2). **(c)** The space of intrinsic growth rates (\mathbf{r}) for the same system shown in (a) and (b) colored according to the distance to closest border ($\min\{d_b\}$) of the feasibility domain, which are indicated as black curves. Note that \mathbf{r} -vectors on the feasibility domain are normalized to unit norm (i.e., $\|\mathbf{r}\| = 1$). **(d)** The same space of intrinsic growth rates, but colored according to the distance to closest vertex ($\min\{d_v\}$) of the feasibility domain.

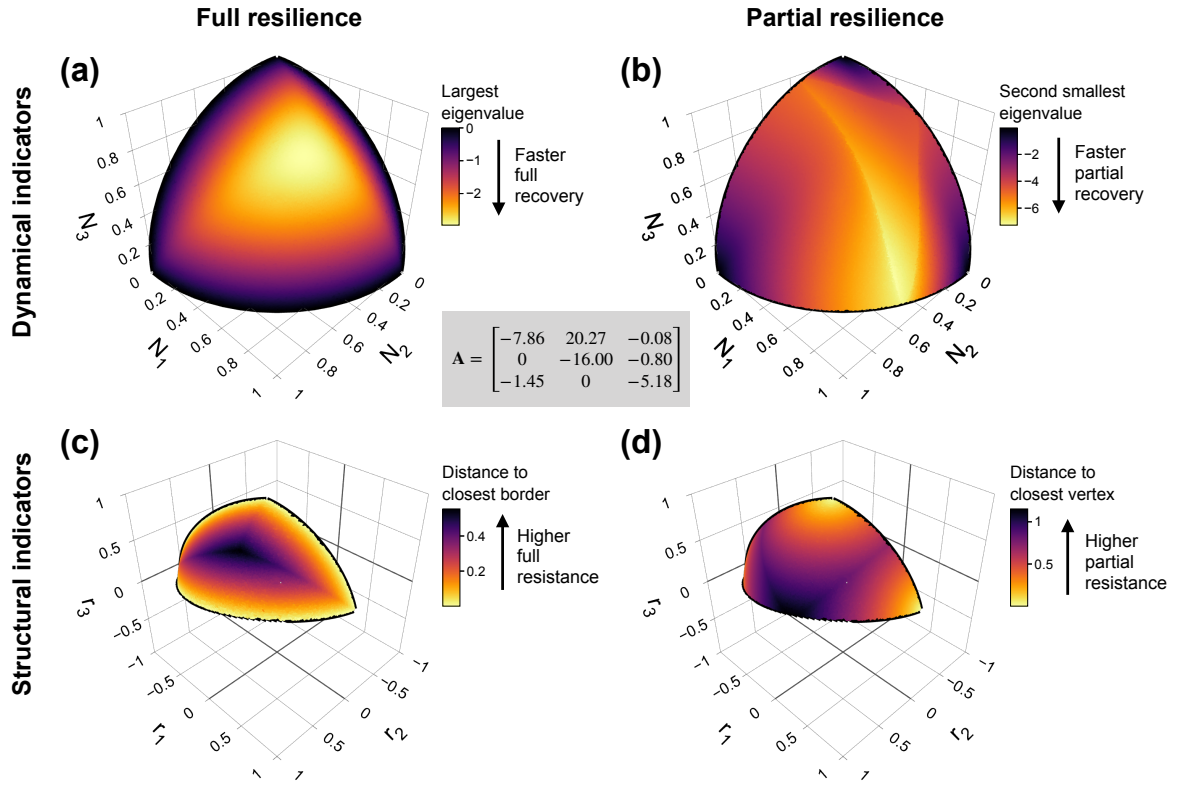


Figure S10: Dynamical and structural indicators of full and partial resilience in a competition/antagonistic microbial system (system 9: Pa-Pci-Pv; Tables S1 and S3). **(a)** The 3-dimensional space of species abundances at equilibrium (\mathbf{N}^*) colored according to the largest eigenvalue of the Jacobian matrix (λ_1). The interaction matrix \mathbf{A} of this 3-species system is shown in the center of the figure. Note that this space corresponds to the positive orthant of the unit sphere (i.e., $\|\mathbf{N}^*\| = 1, N_i^* > 0 \forall i$). **(b)** The same space of species abundances, but colored according to the second smallest eigenvalue of the Jacobian matrix (λ_2). **(c)** The space of intrinsic growth rates (\mathbf{r}) for the same system shown in (a) and (b) colored according to the distance to closest border ($\min\{d_b\}$) of the feasibility domain, which are indicated as black curves. Note that \mathbf{r} -vectors on the feasibility domain are normalized to unit norm (i.e., $\|\mathbf{r}\| = 1$). **(d)** The same space of intrinsic growth rates, but colored according to the distance to closest vertex ($\min\{d_v\}$) of the feasibility domain.

References

Friedman, J., Higgins, L.M. & Gore, J. (2017) Community structure follows simple assembly rules in microbial microcosms. *Nature Ecology and Evolution* **1**, 0109.